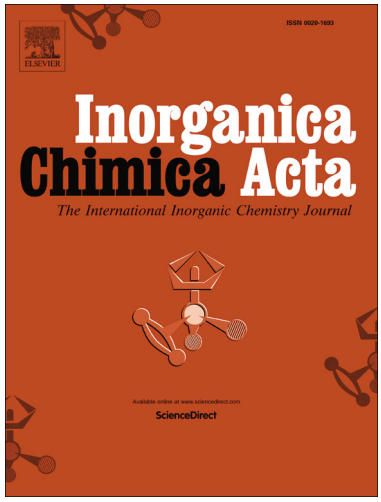

Research paper

Ruthenium(II) complexes of thiosemicarbazones: synthesis, X-ray crystal structures, spectroscopy, electrochemistry, DFT studies and fluoride sensing properties

Bipinbihari Ghosh, Piyali Adak, Subhendu Naskar, Bholanath Pakhira, Partha Mitra, Rupam Dinda, Shyamal Kumar Chattopadhyay

PII: S0020-1693(17)30058-0
DOI: http://dx.doi.org/10.1016/j.ica.2017.01.011
Reference: ICA 17404

To appear in: *Inorganica Chimica Acta*

Received Date: 17 June 2016
Revised Date: 14 December 2016
Accepted Date: 11 January 2017

Please cite this article as: B. Ghosh, P. Adak, S. Naskar, B. Pakhira, P. Mitra, R. Dinda, S.K. Chattopadhyay, Ruthenium(II) complexes of thiosemicarbazones: synthesis, X-ray crystal structures, spectroscopy, electrochemistry, DFT studies and fluoride sensing properties, *Inorganica Chimica Acta* (2017), doi: http://dx.doi.org/10.1016/j.ica.2017.01.011

Ruthenium(II) complexes of thiosemicarbazones: synthesis, X-ray crystal structures, spectroscopy, electrochemistry, DFT studies and fluoride sensing properties

Bipinbihari Ghosh,[a] Piyali Adak,[a] Subhendu Naskar,[b] Bholanath Pakhira,[a] Partha Mitra,[c] Rupam Dinda,[d] Shyamal Kumar Chattopadhyay*[a]

[a]Department of Chemistry, Indian Institute of Engineering Science and Technolgy, Shibpur, Howrah 711103, India

[b]Department of Applied Chemistry, Birla Institute of Technology, Mesra, Ranchi 835215, Jharkhand, India

[c]Department of Inorganic Chemistry, Indian Association for the Cultivation of Science, Jadavpur, Kolkata 700032, India

[d]Department of Chemistry, National Institute of Technology, Rourkela 769008, Orissa, India

*Corresponding Author.

E mail address: shch20@hotmail.com (S.K. Chattopadhyay).

Abstract

Six Ru(II) complexes with formula [Ru(terpy)(L)]X (L = tridentate N,N,S^- donor thiosemicarbazone ligands, X = PF_6^-) have been synthesized and characterized by using standard analytical and spectroscopic techniques. The X-ray crystal structures of the complexes [Ru(terpy)(L^2)]PF_6(**2**) and [Ru(terpy)(L^3)]PF_6(**3**) have been determined. It was found that during complexation the hydroxyimino functionality of the parent ligands is converted to imine, which participates in coordination through the N-atom. The complexes are found to undergo two quasi-reversible oxidations in the positive potential window (0 to +0.8 V) and three successive quasi-reversible/ irreversible reductions in the negative potential window (0 to −2 V). The fluoride sensing properties of all the complexes have been studied in solution using absorption spectra and ^{1}H NMR studies, as well as by cyclic voltammetric (CV) measurements. From the absorption titration studies the association constants and detection limit values of fluoride by the complexes have been determined. The association constant values were found to be reasonably

high ($\log K_a > 5$) for complexes **3**-**6**, and these values are one order of magnitude greater than those observed for the corresponding free thiosemicarbazones. The selective fluoride sensing properties of all the complexes have also been signaled by the development of vivid colors visible with the naked eye.

Keywords: Ru(II) complexes, Thiosemicarbazone, Cyclic voltammetry, X-ray structure, DFT calculations, F^- sensing properties

1. Introduction

Thiosemicarbazones are an important class of N, S-donor ligands, with the free ligands, as well as their metal complexes showing variety of biological activities, including anticancer, antibacterial, antimalarial, antifungal and anti-HIV activities [1-10]. Though coordinated thiosemicarbazones usually form five membered chelate rings [6-12], coordinating through imine nitrogen and the sulfur atom, there are quite a few examples, mainly involving Ru(II) as the metal center, where four membered chelate rings are stabilized, the coordinating atoms being the sulfur and the deprotonated hydrazinic nitrogen [13-17]. The relative stability of the four membered versus five membered chelate rings have been found to depend on number of factors, including nature of the coligands, solubility of the complexes, H-bonding interactions and packing forces[13]. Thus, reaction of $Ru(PPh_3)_3Cl_2$ with pyridine-2-aldehyde (4-cyclohexyl)thiosemicarbazone gave $[Ru(PPh_3)_2(H_2N\text{^}S)_2]^{2+}$, where $H_2N\text{^}S$ stands for the nondeprotonated thiosemicarbazone ligand which coordinates through imine N (N^1, see scheme-1) and thione sulfur, forming five membered chelate ring, whereas reaction of the same Ru(II) precursor with pyridine-2-aldehyde thiosemicarbazone and pyridine-2-aldehyde (4-alkyl/aryl)thiosemicarbazones in presence of Et_3N gave complexes of type $[Ru(PPh_3)_2(HN\text{^}S)_2]$, where HN^S is monoanionic form of thiosemicarbazone, coordination through deprotonated N^2 nitrogen and the sulfur atoms, forming four membered chelate ring [18,19, 20d]. Again, thiosemicarbazones of thiophen-2-aldehyde as well as benzaldehyde form four membered chelate rings when the coligands are two *cis*-PPh_3 groups or a bidentate 1,4-

bis(diphenylphosphino)butane ligand, but when bi(diphenylphosphino)methane is used as coligand the same thiosemicarbazones form five membered chelate rings, along with orthometallation of the heterocyclic/ aromatic ring [13,15,16,20]. It was also shown that complexes of the type $[Ru(PPh_3)_2(HN\hat{}S)_2]$ may act as metallo-ligand and can form oligonuclear complexes like $[(Ph_3P)_2Ru^{II}(N\hat{}S)_2Cu^{II}{}_2Cl_2]$, $[\{(Ph_3P)_2Ru^{II}(N\hat{}S)_2\}_4Ni^{II}{}_4]^{4+}$ (N^S = dideprotonated pyridine-2-aldehyde thiosemicarbazone or salicyl aldehyde thiosemicarbazone, deprotonations occurring from N^2 and N^4 nitrogen atoms) [14d,19]. Thiosemicarbazides and thiosemicarbazones are known to be redox non-innocent ligands [7,24,25]. It was also shown that Ru(II)-thiosemicarbazone complexes possess interesting electronic structures as there are appreciable mixing between the Ru(II) orbitals and the ligand orbitals in these complexes. Therefore, thiosemicarabzone complexes of Ru(II) continues to be a fertile area of investigation with structural diversity and intriguing electronic structures as noted above along with the revelations of its potential medicinal applications [5-10, 23]. These developments have been summarized in recent reviews [17, 24].

Anions like acetate, phosphates, and fluoride play important roles in biology [25]. Therefore design of specific sensors for each of these anions has emerged as an important and active area of research in recent times [26]. Fluoride ion has important structural role in maintaining integrity of structures of bones and teeth enamel. However, excess of fluoride, often contaminated with drinking water, causes health hazard such as fluorosis, urolithiasis, and cystic fibrosis [27,28]. Compounds containing N-H protons, such as imidazoles, pyrazoles, amides, thiourea and urea derivatives have been extensively used as chromogenic and fluorogenic sensors for anions, particularly for fluoride ion [29-33]. This is because of the ability of the N-H proton to enter into strong hydrogen bonding interaction with anions like F^-. 4-aryl substituted thiosemicarbazones possess two N-H protons in the nondeprotonated state and on deprotonation, particularly during chelation, one N-H proton remains in the thiosemicarbazide fragment, whose acidity can be controlled by substitution on the adjacent aromatic ring as well as by changing the metal ion to which it is coordinated. As a result phenylthiourea derivatives in general, and thiosemicarbazones in particular, are now subject of intense investigations as anion receptor, particularly of fluoride [32,33-35]. However, a major problem with many of the reported sensors of fluoride ions is that they often also sense acetate ions [29b-h, 30c-d, 33b-c, 34, 35]. Therefore, design of new sensors with high specificity for fluoride ion is a highly desirable goal. In this

regard, we thought that ternary complexes of thiosemicarbazones with preformed Ru(II)-polypyridyl core are likely to be good chromogenic platform for F^- detection, where the thiosemicarbazone fragment will act as sensor unit and Ru(II)-polypyridyl fragment will be the reporter unit. Towards this goal, we report in this paper six mixed ligand complexes of Ru(II) containing terpyridyl and six tridentate thiosemicarbazones and the F^- sensing properties of these Ru(II) complexes.

In recent years we have been investigating in our laboratory the redox non-innocent behavior of thiosemicarbazones and the extent of coupling of the metal and thiosemicarbzone orbitals in Ruthenium(II)-thiosemicarbazone complexes [13,15,16]. In this work also, we have devoted some of our attention to this interesting aspect of Ru(II)-thiosemicarbazone chemistry, apart from focusing on the primary objective the work of identifying metal complexes of thiosemicarbazones as fluoride selective sensors. As an interesting aside, we also report here a relatively rare conversion of oxime functionality of the ligands to metal coordinated imine moiety.

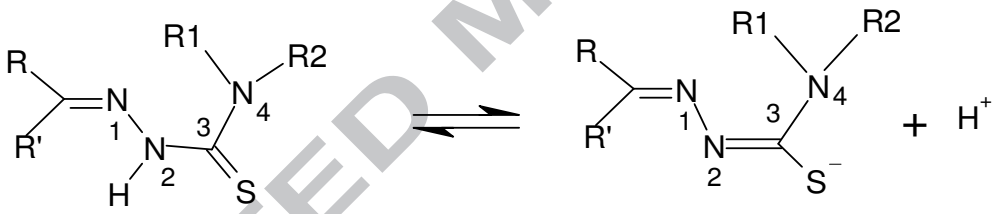

Scheme 1: Protonated and deprotonated forms of thiosemicarbazone ligands along with the atom numbering scheme.

2. Experimental

2.1. Materials and methods

Diacetyl monooxime was purchased from Aldrich and triethylenetetramine was purchased from E. Merck. All other chemicals and solvents were of reagent grade and used as such. $Ru(terpy)Cl_3$ was prepared following a published procedure [36]. Solvents for spectroscopic and cyclic voltammetry studies were of HPLC grade obtained from Merck or Aldrich**.** Elemental analyses were performed on a Perkin–Elmer 2400 C, H, N analyzer. Infrared spectra were recorded as KBr pellets on a JASCO FT-IR-460 spectrophotometer. UV–Vis spectra were recorded using a JASCO V-530 spectrophotometer. Electrochemical data of 1-2 mM CH_3CN solutions of the

complexes were collected using a CH1106A potentiostat. A three electrode configuration, consisting of a glassy carbon working electrode and a Pt-wire auxiliary electrode, Ag/AgCl, KCl(sat) reference electrode and TEAP as supporting electrolyte, were used. The potentials were calibrated against the ferrocene/ferrocenium couple (E^0 = 0.44 V). ^{1}H and ^{13}C NMR spectra were recorded on a Bruker AVANCE DPX 400 MHz spectrometer using, $Si(CH_3)_4$ as internal standard. ESI-MS spectra of the samples were recorded on JEOL JMS 600 instrument.

2.2. Synthesis of ligands

The ligands (Scheme 1), (E)-1-(3-hydroxyiminobutan-2-ylidene)-4-p-tolylthiosemicarbazide (**L^1H'**), (E)-1-(3-hydroxyiminobutan-2-ylidene)-4-phenylthiosemicarbazide (**L^2H'**), (E)-4-(4-chlorophenyl)-1-(3-hydroxyiminobutan-2-ylidene)thiosemicarbazide (**L^3H'**), (E)-4-(4-fluorophenyl)-1-(3-hydroxyiminobutan-2-ylidene)thiosemicarbazide (**L^4H'**), (E)-4-(4-bromophenyl)-1-(3-hydroxyiminobutan-2-ylidene)thiosemicarbazide (**L^5H'**) and (E)-1-(3-hydroxyiminobutan-2-ylidene)-4-(4-methoxyphenyl)thiosemicarbazide (**L^6H'**) were prepared using the corresponding aryl amines by the published procedure [37-39].

2.3. Synthesis of Complexes

The complexes (Scheme 2) $[Ru(terpy)L^1]PF_6$ (**1**), $[Ru(terpy)L^2]PF_6{\cdot}3H_2O$ (**2**), $[Ru(terpy)L^3]PF_6{\cdot}MeOH$ (**3**), $[Ru(terpy)L^4]PF_6{\cdot}2H_2O{\cdot}MeOH$ (**4**), $[Ru(terpy)L^5]PF_6{\cdot}H_2O$ (**5**) and $[Ru(terpy)L^6]PF_6.H_2O$ (**6**) were synthesized following a general procedure outlined below for complex **1**, using the appropriate thiosemicarbazone.

*2.3.1. $[Ru(terpy)L^1]PF_6$ (**1**)*

To a 50 ml ethanolic solution of the L^1H (132.5 mg, 0.5 mmol), Et_3N (50 mg, 0.5 mmol) was added, followed by the addition of solid $Ru(terpy)Cl_3$ (220.25 mg, 0.5 mmol) and the reaction mixture was refluxed with continuous stirring for 8 hours; the solution was cooled and solid NH_4PF_6 was then added to the brown red reaction mixture and filtered. The filtrate was evaporated to dryness on rotary evaporator. The entire crude product was then purified by silica gel column chromatography. An intense reddish brown band was eluted with chloroform–methanol mixture (9:1). Evaporation of the solvent and recrystallization from 1:1 chloroform–methanol solution leads to deep brown crystals.

Yield: 57%. *Anal.* Calc. for $C_{27}H_{26}F_6N_7PRuS$ (Found): C, 44.63 (44.51); H, 3.61 (3.48); N, 13.49 (13.38)%. ESI-MS (positive, MeOH) *m/Z* = 582.07 (100%) $[M–PF_6]^+$. UV−Vis [MeCN; λ_{max}/nm

(ε/ M^{-1} cm^{-1})]: 271 (81280), 312 (87620), 381 (46736), 498 (37336), 661 (3756). ^{1}H-NMR (DMSO-d_6): δ (ppm) (see Scheme 2 for proton numbering): 9.79 (s, 1H, H1), 9.51 (s, 1H, H2), 8.76 (d, 2H, J=8 Hz, H8), 8.51 (d, 2H, J=8 Hz, H5), 8.13 (m, 3H, 1H3+2H4), 8.02 (m, 2H, H6), 7.68 (d, 2H, J=8.4 Hz, H9), 7.59 (m, 2H, H7), 7.12 (d, 2H, J=8.4 Hz, H10), 2.69 (s, 3H, H11), 2.25 (s, 3H, 4-(CH_3)Ph), 2.19 (s, 3H, H12). ^{13}C{^{1}H} NMR (DMSO-d_6): δ(ppm): 177.81, 157.54, 154.54, 153.41, 136.6, 133.33, 131.74, 129.33, 128.08, 123.54, 122.59, 120.63, 49.07, 31.16, 22.95, 20.84, 15.87. Selected IR bands (cm^{-1}): 3315 (ν_{N-H}), 1596 ($\nu_{C=N}$).

*2.3.2. [Ru(terpy)L^2]PF_6·3H_2O (**2**)*

Yield: 59%. Anal. Calc. for $C_{26}H_{30}F_6N_7O_3PRuS$ (Found): C, 38.96 (40.28); H, 3.01 (3.21); N, 11.78 (12.05)%. ESI-MS (positive, MeOH) m/Z = 567.79 (100%) [M−PF_6−$CHCl_3$]$^{+}$. UV−Vis [MeCN; λmax/ nm (ε/ M^{-1} cm^{-1})]: 272 (77868), 311 (87210), 374 (48616), 498 (36046), 665 (3362). ^{1}H-NMR (DMSO-d_6): δ (ppm): 9.82 (s, 1H, H1), 9.57 (s, 1H, H2), 8.77 (d, 2H, J=8 Hz, H8), 8.65 (d, 2H, J=8 Hz, H5), 8.11 (m, 3H, 1H3+2H4), 8.02 (m, 2H, H6), 7.82 (d, 2H, J=8 Hz, H9), 7.59 (m, 2H, H7), 7.32 (m, 2H, H10), 6.97 (m, 1H, 4-(H)Ph), 2.71 (s, 3H, H11), 2.20 (s, 3H, H12). ^{13}C{^{1}H} NMR (DMSO-d_6): δ(ppm): 177.65, 176.84, 157.54, 154.56, 153.45, 141.37, 136.63, 133.33, 128.95, 128.09, 123.55, 122.77, 122.62, 120.52, 79.59, 22.97, 15.91. Selected IR bands (cm^{-1}): 3421 ν_{O-H}, 3315 (ν_{N-H}), 1596 ($\nu_{C=N}$).

*2.3.3. [Ru(terpy)L^3]PF_6·MeOH (**3**)*

Yield: 57%. Anal. Calc. for $C_{27}H_{26}ClF_6N_7OPRuS$ (Found): C, 41.64 (41.52); H, 3.34 (3.27); N, 12.59 (12.44)%. ESI-MS (positive, MeOH) m/Z = 601.73 (100%) [M−PF_6−MeOH]$^{+}$. UV−Vis [MeCN; λ_{max}/ nm (ε/M^{-1} cm^{-1})]: 271 (89960), 311 (101196), 375 (59768), 499 (46122), 662 (4170). ^{1}H-NMR (DMSO-d_6): δ (ppm): 9.86 (s, 1H, H1), 9.69 (s, 1H, H2), 8.77 (d, 2H, J=8 Hz, H8), 8.65 (d, 2H, J=8 Hz, H5), 8.14 (m, 3H, 1H3+2H4), 8.02 (m, 2H, H6), 7.84 (d, 2H, J=8.8 Hz, H10), 7.59(m, 2H, H7), 7.37 (d, 2H, J=8.8 Hz, H9), 2.71 (s, 3H, H11), 2.02 (s, 3H, H12). ^{13}C{^{1}H} NMR (DMSO-d_6): δ(ppm): 177.77, 157.52, 154.56, 154,153.50, 140.29, 136.69, 133.45, 128.79, 128.12, 126.31, 123.57, 122.64, 121.99, 22.98, 15.97. Selected IR bands (cm^{-1}): 3414 (ν_{O-H}), 3310 (ν_{N-H}), 1588 ($\nu_{C=N}$).

*2.3.4. [Ru(terpy)L^4]PF_6·2H_2O·MeOH(**4**)*

Yield: 56%. Anal. Calc. for $C_{27}H_{31}F_7N_7O_3PRuS$ (Found): C, 40.60 (40.49); H, 3.91 (3.83); N, 12.28 (12.19)%. ESI-MS (positive, MeOH) m/Z = 586.01 (100%) [M−PF_6−2H_2O−MeOH]$^{+}$. UV−Vis [MeCN; λmax/ nm (ε/ M^{-1} cm^{-1})]: 272 (82900), 311 (99206), 374 (55266), 498

(43960), 664 (4106). ^{1}H-NMR (DMSO-d_6): δ (ppm): 9.83 (s, 1H, H1), 9.61 (s, 1H, H2), 8.77 (d, 2H, J=8 Hz, H8), 8.65 (d, 2H, J=8.4 Hz, H5), 8.14 (m, 3H, 1H3+2H4), 8.02 (m, 2H, H6), 7.82 (m, 2H, J=8.4 Hz, H10), 7.59 (m, 2H, H7), 7.18 (m, 2H, H9), 2.70 (s, 3H, H11), 2.20 (s, 3H, H12). ^{13}C{^{1}H} NMR (DMSO-d_6): δ(ppm): 177.65, 157.54, 154.58, 153.46, 137.90, 136.64, 133.36, 128.09, 123.55, 122.62, 122.12, 115.55, 115.33, 79.59, 21.95, 15.90. Selected IR bands (cm^{-1}): 3453 (ν_{O-H}), 3315 (ν_{N-H}), 1605 ($\nu_{C=N}$).

*2.3.5. [Ru(terpy)L^5]PF_6·H_2O (**5**)*

Yield: 61%. Anal. Calc. for $C_{26}H_{25}BrF_6N_7OPRuS$ (Found): C, 38.58 (38.46); H, 3.11 (3.01); N, 12.11 (12.01)%. ESI-MS (positive, MeOH) m/Z = 547.98 (100%) $[M-PF_6-H_2O]^+$. UV−Vis [MeCN; λmax/ nm (ε/ M^{-1} cm^{-1})]: 270 (88848), 312 (95246), 375 (56356), 498 (42670), 659 (3860). ^{1}H-NMR (DMSO-d_6): δ (ppm): 9.85 (s, 1H, H1), 9.67 (s, 1H, H2), 8.76 (d, 2H, J=8.4 Hz, H8), 8.65 (d, 2H, J=8 Hz, H5), 8.13 (m, 3H, 1H3+2H4), 8.02 (m, 2H, H6), 7.78 (d, 2H, J=8.8 Hz, H10), 7.59(m, 2H, H7), 7.49 (d, 2H, J=8.8 Hz, H9), 2.71 (s, 3H, H11), 2.25 (s, 3H, H12), 2.20 (s, 3H). ^{13}C{^{1}H} NMR (DMSO-d_6): δ(ppm): 207.24, 177.78, 157.51, 154.56,153.50, 140.69, 136.70, 133.46, 131.68, 128.12, 123.57, 122.64, 122.42, 114.35, 31.15, 22.98, 15.96. Selected IR bands (cm^{-1}): 3408 (ν_{O-H}), 3315 (ν_{N-H}), 1599 ($\nu_{C=N}$).

*2.3.6. [Ru(terpy)L^6]PF_6·H_2O (**6**)*

Yield: 59%. Anal. Calc. for $C_{27}H_{28}F_6N_7O_2PRuS$ (Found): C, 42.63 (42.55); H, 3.71 (3.62); N, 12.89 (12.77)%. ESI-MS (positive, MeOH) m/Z = 598.08 (100%) $[M-PF_6-H_2O]^+$. UV−Vis [MeCN; λmax/ nm (ε/ M^{-1} cm^{-1})]: 271 (98758), 312 (10678), 386 (59510), 498 (50466), 664 (4666). ^{1}H-NMR (DMSO-d_6): δ (ppm): 9.78 (s, 1H, H1), 9.49 (s, 1H, H2), 8.78 (d, 2H, J=8 Hz, H8), 8.67 (d, 2H, J=8 Hz, H5), 8.15 (m, 3H, 1H3+2H4), 8.04 (m, 2H, H6), 7.74 (d, 2H, J=8 Hz, H10), 7.61 (m, 2H, H7), 6.92 (d, 2H, J=9.2 Hz, H9), 3.74 (s, 3H, 4-(OCH_3)Ph), 2.74 (s, 3H, H11) , 2.21 (s, 3H, H12). ^{13}C{^{1}H} NMR (DMSO-d_6): δ(ppm): 177.48, 157.57, 155.21, 154.60, 153.36, 136.55, 134.83, 133.18, 128.04, 123.51, 122.56, 120.10, 114.07, 79.72, 55.68, 22.92, 15.81. Selected IR bands (cm^{-1}): 3421 (ν_{O-H}), 3286 (ν_{N-H}), 1593 ($\nu_{C=N}$).

2.4. X-ray crystallography

Single crystal X-ray data were collected for **2** and **3** at 150 (2) and 293(2) K respectively, on a Bruker AXS SMART APEX-II CCD area detector diffractometer using graphite monochromated Mo-Kα radiation. Data were corrected for absorption effects using the numerical method SADABS [40], solved by direct methods and refined by full matrix least squares on F^2 using

SHELX-97 [41]. All non-hydrogen atoms were refined with anisotropic displacement parameters. A summary of the crystallographic data is presented in Table 1. Important bond distances and bond angles are collected in Table 2. Crystallographic data has been deposited at CCDC with deposition no. 1448038 for **2** and 1448039 for **3**.

Table 1. Crystal data and structure refinement parameters for **2** and **3**.

Compounds	**2**	**3**
Formula	C_{27} H_{25} Cl_3 F_6 N_7 P Ru S	C_{27} H_{26} Cl F_6 N_7 O P Ru S
Formula weight	831.99	778.10
Wavelength (Å)	0.71073	0.71073
Temperature	150(2)	293(2)
Crystal system	triclinic	triclinic
Space group	P -1	P -1
a (Å)	8.685(4)	11.1857(19)
b (Å)	12.008(5)	12.259(2)
c(Å)	16.603(7)	12.351(2)
α(°)	72.086(8)	79.834(4)
β(°)	85.233(9)	70.415(4)
γ(°)	82.114(9)	84.421(4)
Density (calculated) (g cm^{-3}), Z	1.695, 2	1.647, 2
μ(mm^{-1})	0.906	0.773
F*(000)*	832	782
Reflections collected: total, unique	15403, 5745	15199, 5527
Max. and min. transmission	0.897, 0.850	0.884, 0.857
Observed data [I>2σ(I)]	5088	4592
R(int)	0.0237	0.0378
R1, wR2 [I>2σ(I)]	0.0531,0.1521	0.0385,0.0900
R1, wR2 (all data)	0.0593, 0.1598	0.0497, 0.0969
Data/restraints/parameters	5745/0/417	5527/0/410
Goodness-of-fit (GOF) on F^2	1.030	1.05
Largest difference in peak and hole (e $Å^{-3}$)	–0.893, 1.197	–0.498, 0.658

2.5. Computational Details

DFT calculations were performed using Gaussian 03 package (Revision A.02) [42]. The molecular orbitals were visualized using Gauss View software. Geometry optimizations, single point calculations, and population analysis of the molecular orbitals were carried out at the density functional theory (DFT) level with B3LYP hybrid exchange functional [43] and the nonlocal correlation provided by the Lee and the Vosko et al. For H, C, N, and O atoms 6-31G*+

basis set [44] were used. The LANL2DZ [45] basis set and LANL2DZ pseudopotentials of Hay and Wadt [46] were used for the Ru atom. The initial geometry of the complexes **2** and **3** were taken from their crystal structures and they were optimized without any symmetry constraints, in MeCN solvent, using CPCM model [47].

For time dependent density functional theory (TD-DFT) calculations, same basis set with the CPCM model were used, taking acetonitrile as the solvent. Singlet excited states were calculated based on the singlet ground-state geometry. The lowest 40 singlet excited states, with oscillator strengths greater than 0.01, were considered for TD-DFT calculations.

2.6. Anion Binding Studies

All the solvents were of HPLC grade and were used without any further purification. The anions used for the titrations were in the form of their tetrabutylammonium salts. Stock solutions of the complexes (5×10^{-4}M), free ligands (1×10^{-3}M) and of tetrabutylammonium salts of the respective anions (2×10^{-4}M) were prepared in HPLC grade acetonitrile and were stored in dark. For absorption measurements, the stock solutions of the complexes and ligands were diluted to 1×10^{-5}M and 5×10^{-5}M respectively. The titration experiments were performed at room temperature (298 K) by placing 2 mL solution of a complex or a ligand in a quartz cuvette of 1-cm path length and various amounts of anions were added incrementally from a micropipette. The association constant of the anion with the complex in the solution was estimated by using the equation (1) and (2) [48,49]

$$[\mathrm{Ru(terpy)(L)}]^{+} + \mathrm{F}^{-} \rightleftharpoons [[\mathrm{Ru(terpy)(L)}]^{+}\cdot\mathrm{F}^{-}]$$

$$K = \frac{[[\mathrm{Ru(terpy)(L)}]^{+}\cdot \mathrm{F}^{-}]}{[\mathrm{Ru(terpy)(L)}]^{+} + [\mathrm{F}^{-}]} \qquad (1)$$

$$\Delta A = \frac{\Delta\boldsymbol{\varepsilon}([\mathrm{S}]+[\mathrm{G}]+1/K_a) \pm (\Delta\boldsymbol{\varepsilon}^2([S]+[G]+1/K_a)^2 - 4\Delta\boldsymbol{\varepsilon}^2[S][G])^{1/2}}{2} \qquad (2)$$

In eqn (2), ΔA represents the change in the initial absorbance of the complexes at 535 nm upon each addition of the fluoride ion and [S] and [G] are the concentrations of the complex and fluoride ion respectively, during the spectrophotometric titrations. The association constant (K_a) and the change in the molar extinction coefficient (Δε) at each concentration of F^- for the complexes are evaluated by the nonlinear curve fitting procedure. The association constants (K_a)

for the complexes are given in Table 7, whereas those for the free ligands are given in Fig. S35 and Table S2.

The cyclic voltammetric (CV) and differential pulse voltammetric (DPV) titrations measurements were carried out at 298 K in HPLC grade degassed acetonitrile solution of the complex **3** (2×10^{-4}M), which was taken as a representative example, and the concentration of the supporting electrolyte (TEAP) was maintained at 0.1 M. For electrochemical titrations, 20 µL aliquots of a tetrabutylammonium salt of the anions (5×10^{-3} M in acetonitrile) were added to a 5 mL solution of **3**.

3. Results and discussions

3.1. Synthesis

The thiosemicarbazone ligands L^1H'–L^6H' were prepared by a procedure described earlier (scheme 2). The syntheses of Ru(II) complexes **1**-**6** were achieved by refluxing equimolar amounts of the corresponding thiosemicarbazone ligand with Ru(terpy)Cl_3 (terpy: 2,2′:6′,2″-terpyridine) and triethylamine in ethanolic solution for 8 hours, followed by anion exchange with ammonium hexafluorophosphate (scheme 3). The crude products were then purified by column chromatography over silica gel using chloroform–methanol (9:1) mixture as the eluent. The compounds were finally recrystallized from chloroform-methanol (1:1) mixture. All the compounds have been characterized by their elemental (C, H, and N) analyses, ESI-MS, IR, UV-vis, ^{1}H- and ^{13}C-NMR spectroscopic measurements, and the results are given in the Experimental Section. Single crystals suitable for X-ray crystallography of **2** and **3** were obtained from the slow evaporation of 1:1 chloroform–methanol mixture.

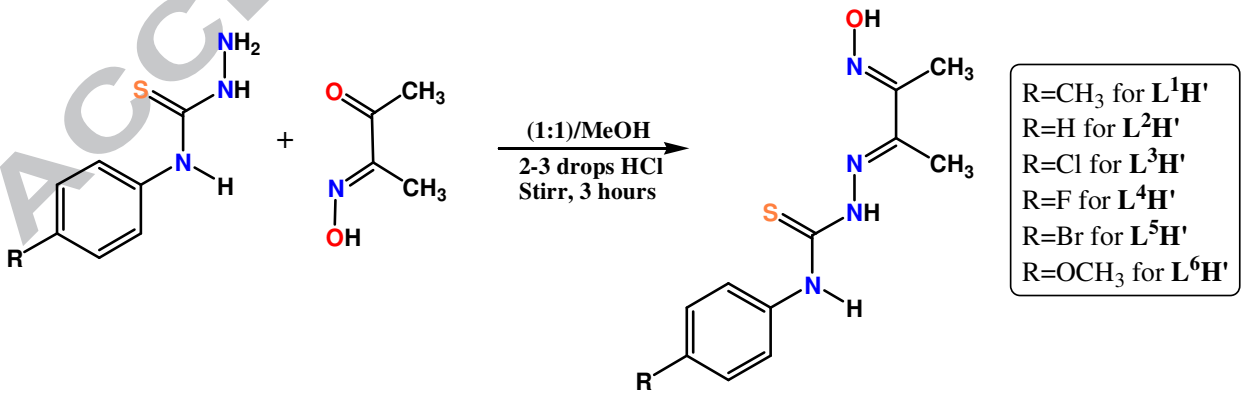

Scheme 2: Schematic representation for the synthesis of the Ligands.

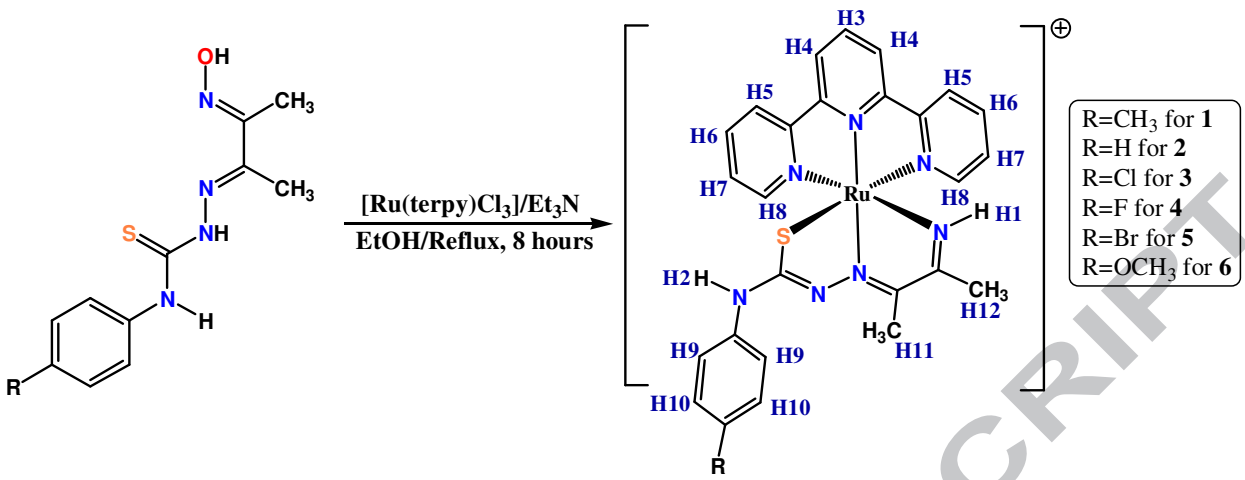

Scheme 3: Schematic representation for the synthesis of the Ru(II) complexes.

During the synthesis of the complexes, ruthenium which was present in +3 oxidation state in the precursor Ru(terpy)Cl_3 is reduced to +2 oxidation state by the ligands. Thiosemicarbazones are known to be good reducing agents and such reduction of Ru(III) to Ru(II) by thisoemicarbazides and thiosemicarbazones have been previously noticed [3-5, 11,12]. The n.m.r. spectra of the complexes indicate that the oxime moiety that is present in the ligands are absent in the complexes. This is further confirmed by the determination of X-ray crystal structures of two of the complexes. Conversion of oximes to imines, and isolation and X-ray structural characterization of the resultant imine complexes was reported earlier where oximes of salicylaldehyde, 2-hydroxy acetophenone and 2-hydroxy napthylaldehyde or aryl azo-oximes were converted to the corresponding imine complexes of Ru(III) and Re(V) [50,51]. Deoxygenation/ reduction of oximes has been found to be effected by oxophilic species like PPh_3, CO, Re(I), Re(III), $SOCl_2$ or reducing agents like citric acid [50-52]. Low-valent electron rich metal ions are also known to convert oxime to imines [53,54]. Thus, in the present case, a combination of electron rich Ru(II) and moderately strong reducing agent thiosemicarbazone, probably act synergistically to reduce the oxime moiety to imine. As a plausible mechanism it may be thought that the initially formed Ru(II) oxime complex undergoes two electron transfer from Ru(II) to oxime forming the Ru(IV) imine complex, which rapidly undergoes reduction by the free thiosemicarabzone ligand to form the Ru(II) imine complex. The relatively low Ru(III)/Ru(II) and Ru(IV)/Ru(III) potentials observed in our complexes (see section 3.7) add strength to our above mechanistic proposition.

3.2. Description of X-ray crystal structure

The molecular structures of complexes **2** and **3** along with the atom numbering schemes are shown in Figs. 1 and 2 respectively. In both the complexes Ru(II) is in a distorted octahedral geometry, coordinated by a tridentate N,N,S-donor thiosemicarbazone ligand and a terpyridyl moiety. In each of these two structures the largest trans angle (174.39(14)° for **2** and 173.43(11)° for **3**) observed involves the endo-nitrogen atom of terpyridyl chelate ring and the hydrazone nitrogen of the thiosemicarbazone moiety (N3-Ru1-N5). The other two trans angles involving the terminal nitrogen atoms of the terpyridyl (N1-Ru1-N2) or the terminal sulfur and imine nitrogen atoms of the thiosemicarbazone ligand (S1-Ru1-N4) lie between 157.58(19)-159.23(9)°. The best least square plane consists of Ru1, S1, N3, N4 and N5, with the r.m.s deviations of the constituent atoms being 0.047(7) Å for **2** and 0.019(3) Å for **3**. The C(26)–S(1) bond distance is 1.747(5) and 1.763(3) Å in complex **2** and **3** respectively, and the corresponding thioamido C(26)–N(6) bond distance is 1.305(6) and 1.313(4) Å for **2** and **3** respectively, which may be compared with the corresponding C-S and C-N bond distances of 1.673(2) and 1.373(2) Å in the free ligand diacetyl monoxime (4-phenyl)thiosemicarabzone [39], clearly indicating that thiosemicarabzone is coordinated in deprotonated thioamide form. The metal ligand bond distances in the thiosemicarbazone fragment is very similar to those observed earlier for Ru(II) complexes of tridentate thiosemicarbazone ligands [6,12,24,55]. The most interesting observation obtained from the X-ray crystal structures is the revelation that the hydroxyimino fragment has been converted to a ketone imine and the later is coordinated to Ru(II) through the imine nitrogen. N-unsubstituted imines, particularly of ketones, are generally unstable and prone to rapid hydrolysis [56] As a result, complexes of such ketone imines are relatively rare in number [12,52,57]. In the DFT optimized structure of the monoanioinic tridentate ligand found in complex **2** (see Fig. S37 and Table S3 in SI), the ketone imine bond distance (C1-N1 distance) is 1.284 Å, while the C1-C2 distance is 1.492 Å. This may be compared with the observed values of the corresponding C22-N4 distances at 1.290(6) Å and 1.295(4) Å in complexes 2 and 3 respectively and C22-C24 distances at 1.446(6) Å in the complex **2** and 1.456 (5) Å in complex **3**, indicating back donation from Ru(II) filled dπ-orbitals to the vacant π*-orbital of the imine ligand. The change in bond lengths in the thiosemicarbazone fragment of the complexes compared to that of the free ligand is indicative of extensive π-delocalization over the ligand backbone.

Fig. 1
Fig. 2

Table 2. Selected bond distances (Å) and angles (°) for **2** and **3**.

2		**3**	
Bond distances			
Ru1–N1	2.061(4)	Ru1–N1	2.063(3)
Ru1–N2	2.056(4)	Ru1–N2	2.061(3)
Ru1–N3	1.974(4)	Ru1–N3	1.974(3)
Ru1–N4	2.035(4)	Ru1–N4	2.047(3)
Ru1–N5	1.997(4)	Ru1–N5	2.004(3)
Ru1–S1	2.350(1)	Ru1–S1	2.378(1)
Bond angles			
N3–Ru1–N5	174.39(14)	N3–Ru1–N5	173.43(11)
N3–Ru1–N4	97.96(15)	N3–Ru1–N4	96.09(11)
N5–Ru1–N4	76.81(15)	N5–Ru1–N4	77.42(11)
N3–Ru1–N1	78.64(19)	N3–Ru1–N1	79.02(12)
N5–Ru1–N1	103.16(17)	N5–Ru1–N1	102.04(12)
N4–Ru1–N1	89.67(15)	N4–Ru1–N1	92.00(12)
N3–Ru1–N2	79.04(18)	N3–Ru1–N2	79.27(12)
N5–Ru1–N2	99.26(16)	N5–Ru1–N2	99.76(11)
N4–Ru1–N2	95.47(15)	N4–Ru1–N2	92.30(11)
N1–Ru1–N2	157.58(19)	N1–Ru1–N2	158.20(12)
N3–Ru1–S1	103.34(11)	N3–Ru1–S1	104.65(8)
N5–Ru1–S1	82.01(10)	N5–Ru1–S1	81.86(8)
N4–Ru1–S1	158.42(12)	N4–Ru1–S1	159.23(9)
N1–Ru1–S1	91.14(11)	N1–Ru1–S1	90.74(8)
N2–Ru1–S1	91.95(12)	N2–Ru1–S1	92.76(8)

3.3. ^{1}H and ^{13}C NMR Spectra

^{1}H and ^{13}C NMR spectra for complexes **1–6** were recorded in DMSO-d_6 at room temperature to confirm the molecular structures of the complexes in solution, and their chemical shift values are given in the Experimental Section and the ^{1}H NMR spectra for complexes **1–6** are shown in Fig. S19. In all the Ru(II) complexes (**1-6**), imine (=N-H) protons and N-H adjacent to the phenyl ring (4-(R)Ph-NH-) are observed at 9.7-9.8 ppm and 9.5-9.6 ppm respectively. The appearance of imime (=N-H) proton as a singlet confirms the conversion of oxime to imine during complexation. Two sets of doublets and three sets of multiplets are observed for coordinated terpyridine group, with almost same chemical shift in all the complexes. Methyl protons of 4-(CH_3)Ph and 4-(OCH_3)Ph, appeared as a singlet at δ2.25 ppm and δ3.74 ppm respectively. Two

methyl protons of diacetyl group observed as singlets at 2.7 ppm and 2.2 ppm, and 4-Phenyl protons show as a multiplet at δ6.97 ppm.

In ^{13}C NMR spectra of all the complexes (**1-6**), twelve non equivalent aromatic carbon atoms along with three aliphatic (C=N) carbon atoms are observed in the region 177.8-79.6 ppm. Two methyl carbon of diacetyl group are found at 22.9 ppm and 15.9 ppm, whereas para- substituted methyl and methoxy carbon atom of **1** and **6** are observed at 22.95 ppm and 55.68 ppm respectively.

3.4. DFT calculations

It was mentioned in the introductory remarks that Ru(II)-thiosemicarbazones possess interesting electronic structures and there is appreciable mixing of Ru(II) dπ-orbitals with thiosemicarabzone orbitals. This makes assigment of oxidation state of the metal ion in these compounds ambiguous. Again, imine complexes, where the imine N is unsubstituted, also show intriguing electronic structures [58-60]. To understand the electronic structures of the complexes as well as to understand the natures of the electronic transitions observed experimentally DFT and TD-DFT calculations were performed on complexes **2** and **3** on their optimized structures in MeCN solution. It was observed that the optimized structures of both the complexes are very similar to those obtained by X-ray crystallography (see Table S4 in SI), except for the fact in the optimized structures in MeCN solution the Ru-N bond lengths are on an average 0.04-0.05Å longer and the Ru-S bond length is about 0.1Å longer than the values observed in the X-ray structures, similar to our earlier observation [61]. The frontier orbitals of both the complexes are very similar and hence the frontier orbitals for complex **2** are shown in Fig. 3, while those for complex **3** are depicted in Fig. S38 (SI). The HOMO contains 47% contribution from Ru(d_π) and 28% contribution from the S(pπ) orbitals, besides some small contribution from imine π-orbital. The HOMO−1 and HOMO−3 also have major contributions from Ru(d_π) orbitlas (62% and 69% respectively), whereas HOMO−2 is predominantly a thiosemicarabzone based π-orbital. The LUMO is a π*-orbital, mainly centered on dimine fragment of the thiosemicarabzone ligand. The LUMO+1 to LUMO+6 are all terpyridine based π*-orbitals. It has been argued that percentage contribution of ruthenium dπ orbitals towards LUMO or LUMO+1, is a measure of metal to ligand back bonding [62-64]. For complexes **2** and **3** it is observed that LUMO has more than 8%, LUMO +1 has more than 7% contribution from the Ru-orbitals, indicating substantial metal to ligand back bonding.

Fig. 3

3.5. IR Spectra

IR spectra of all the complexes are given in Fig S20 and selected i.r. bands are listed in experimental section. Oxime to imine conversion occurs during complexation with Ru(terpy)Cl_3, so a broad band ~3410 cm^{-1} in most of the complexes is due to the ν_{O-H} vibration of the water molecule or MeOH in the crystal lattice. A sharp band ~3315 cm^{-1} overlapping with the broad band mentioned above in all the complexes indicates the presence of N–H bond in the coordinated imine fragment [65]. Bands at ~840-850 cm^{-1} in all the complexes are attributed to $[PF_6]^-$. The $\nu_{C=N}$ stretching frequency is found at 1590 cm^{-1} in all the Ru(II) complexes (**1-6**).

3.6. Electronic Spectra

The electronic spectra of the complexes consist of several intense bands in the visible and UV region (Fig. 4). Two very strong bands at 270 and 311 nm, with molar extinction coefficients grater that 80,000 M^{-1} cm^{-1} are assigned to ligand centered transitions. Two less intense bands at 381 and 498 nm are assigned to metal to terpy charge transfer transitions. A broad shoulder centered on 660 nm is probably due to a MLCT transition involving diimine fragment of the thiosemicarbazone ligand.

Fig. 4

Table 3. Electronic spectral data for the complexes

Complex	**λ/nm (ε/M^{-1} cm^{-1})**
1	271 (81280), 312 (87620), 381 (46736), 498 (37336), 661 (3756)
2	272 (77868), 311 (87210), 374 (48616), 498 (36046), 665 (3362)
3	271 (89960), 311 (101196), 375 (59768), 499 (46122), 662 (4170)
4	272 (82900), 311 (99206), 374 (55266), 498 (43960), 664 (4106)
5	270 (88848), 312 (95246), 375 (56356), 498 (42670), 659 (3860)
6	271 (98758), 312 (10678), 386 (59510), 498 (50466), 664 (4666)

TD-DFT calculations on complexes **2** and **3** were performed for better understanding of the nature of the transitions responsible for the observed electronic spectra. The results of the TD-DFT calculations are given in Table 4. The broad shoulder at around 660 nm has contribution from HOMO to LUMO transition and the calculated peak position is at 635 and 638 nm for complex **2** and **3** respectively; it also has contribution from HOMO to LUMO+1, with calculated peaks at 611 nm (for **2**) and 606 nm (for **3**). Since LUMO is a diimine based π^*-orbital of the

thiosemicarabzone ligand and HOMO is predominantly a Ru d_{π}-orbital with appreciable contribution from Sp_{π}-orbital, so the HOMO to LUMO transition is mainly MLCT (involving π*-diimine of thiosemicarbazone) in nature with some degree of ILCT (intra-ligand charge transfer involving Sp_{π} to diimine-π* fragment of thiosemicarbazone) character. The HOMO to LUMO+1 transition is similarly mainly MLCT (involving π*-terpy orbiltal) and to some extent LLCT (ligand to ligand charge tranfer involving Sp_{π} to π*-terpy) transition. The band observed at 498 nm is mainly due to HOMO−1 to LUMO+1 transition, and hence it can be described as MLCT transition involving π*-terpy orbital. The major contribution towards the intensity of the band at 380 nm is due to HOMO−2 to LUMO transition, though it has also contributions from HOMO−2 to LUMO+2 (for **2**) and HOMO to LUMO+3 (for **3**) transitions. The HOMO−2 to LUMO transition should be considred as ILCT (aromatic amine-π fragment to diimine-π* fragment of the thiosemicarbazone ligand), while HOMO−2 to LUMO+2 is a ligand to ligand charge transfer transition (LLCT from thiosemicarbazone to terpy) and HOMO to LUMO+3 is made up of MLCT involving π*-terpy orbiltal and to some extent LLCT (involving charge tranfer from Sp_{π}-thiosemicrabazone to π*-terpy).

Table 4. Vertical excitations with band position, oscillator strength and character assignment

Complex	**Experimental wave length (nm)**	**Calculated wave length (nm)**	**Oscillator strength (f)**	**Contributing orbital(s)**	**Percentage (%)**
2	272	278.85	0.0716	H-6→L+2 H-5→L+2	25% 56%
	311	300.73	0.2553	H-6→L+1 H→L+5	34% 47%
		301.93	0.1818	H-6→L+1 H→L+5	37% 41%
	374	376.88	0.0592	H-2→L+2	94%
		389.61	0.2704	H-2→L	74%
	498	448.28	0.2119	H-1→L+1	77%
		513.34	0.0005	H-1→L	90%
	665	611.32	0.0087	H→L+1	98%

		634.70	0.0046	H→L	92%
3	271	278.56	0.0943	H-5→L+2	75%
		283.31	0.0179	H-6→L+2	54%
	311	299.74	0.1161	H→L+7	75%
		301.39	0.3299	H-5→L+1	61%
		308.12	0.0318	H-3→L+4	65%
	375	373.47	0.0438	H→L+3	97%
		389.02	0.3315	H-2→L	76%
	499	447.18	0.2325	H-1→L+1	75%
		516.68	0.0005	H-1→L	93%
	662	606.54	0.0088	H→L+1	98%
		638.39	0.0048	H→L	94%

3.7. Electrochemical studies

On the positive side of the Ag/AgCl electrode, complexes **1**-**6** show two quasi-reversible oxidations at 0.5 V and 0.7 V (Fig. 5, Table 5) which are assigned to Ru(III)/Ru(II) and Ru(IV)/Ru(III) couples respectively. Both the couples have ΔE_p value of approximately 65-95 mV and $i_{p.a.}/i_{p.c}$ value 1.4-1.6, indicating electrochemical and chemical quasi-reversibility of these couples. Since the DFT calculations show there is appreciable metal-ligand mixing in the HOMO and HOMO−1, so it should be kept in mind that the above mentioned oxidations cannot be pure metal based oxidations and they involve appreciable charge transfer from the ligand as well. At more positive potential, at around 1.4-1.7 V, two more irreversible oxidations with much higher anodic peak current is observed, which might be attributed to ligand centred oxidations. On the negative side of the reference electrode there are three quasi-reversible/ irreversible reductions at −1.40, −1.60 V and −1.90 V, the first peak is assigned to addition of electron to the diimine fragment of the thiosemicarbazone ligand, whereas the other two peaks are due to electron addition to the π*-orbitals of terpy.

Fig. 5

Table 5. Cyclic voltammetry and differential pulse voltammetry data[a] of complexes **1**-**6** in MeCN solutions.

Complex	E^0/V (ΔE_p/mV) values[b]	DPV

1	0.49(66), 0.73(72), 1.47, 1.72, -1.39, -1.65, -1.98	0.47, 0.71, 1.37, 1.71, -1.49, -1.62, -1.92
2	0.48(75), 0.71(91), 1.45, 1.67, -1.37, -1.61, -1.95	0.45, 0.68, 1.33, 1.58, -1.52, -1.88
3	0.52(65), 0.71(75), 1.45, 1.64, -1.38, -1.60, -1.95	0.49, 0.68, 1.35, 1.55, -1.27, -1.56, -1.89
4	0.50(65), 0.74(69), 1.43, 1.63, -1.33, -1.59, -1.94	0.47, 0.71, 1.32, 1.53, -1.42, -1.62, -1.92
5	0.52(70), 0.71(80), 1.44, 1.64, -1.33, -1.57, -1.94	0.49, 0.69, 1.34, 1.54, -1.33, -1.60, -1.92
6	0.48(62), 0.71(65), 1.29, 1.65, -1.36, -1.70, -1.99	0.45, 0.68, 1.19, 1.55, -1.41, -1.60, -1.91

[a] Scan rate is 100 mV/s. [b] Potentials are referred against Ag/AgCl electrode.

4. Anion-Sensing Studies

4.1. Color Changes of the Receptors in Solution upon Interaction with Anions

The initial assessment of anion sensing abilities of the complexes (**1**-**6**) were on a qualitative basis by visual examination of the anion-induced color changes in acetonitrile solutions (5×10^{-5} M) before and after the addition of an anions such as F^-, Cl^-, Br^-, I^-, OAc^-, SCN^-, HSO_4^- and $H_2PO_4^-$. Tetrabutylammonium salts of the anions were used to observe the visual color changes. The photograph in Fig. 6 shows the dramatic colour changes of complex **3** in the presence of one equivalent of fluoride ion, in contrast the other anions (up to 5 equivalents) induce almost no change in colour. The other three complexes **4**, **5** and **6** also show similar type of color changes with fluoride ion but somewhat less intense color is obtained in case of complexes **1** and **2**. This implies that the complexes **3**-**6** are particularly effective as F^- ion selective colorimetric sensors.

Fig. 6

4.2. ^{1}H NMR Spectral Changes of the Receptors upon Interaction with Anions

To prove the interaction of the complexes (**1-6**) with fluoride ion, ^{1}H NMR titrations of **3** were carried out with additions of increasing amounts of tetrabutyl ammonium fluoride (TBAF) to DMSO solution. Typically a 5.0×10^{-3} M solutions of **3** in DMSO-d_6 were titrated with F^- ion up to 2 equivalents. Fig. 7 shows that the two N–H protons, imine (=N–H) and secondary amine adjacent to the phenyl ring (4-(Cl)Ph-NH-) appeared as a singlet at 9.86 ppm and 9.69 ppm respectively in the ^{1}H NMR spectrum of the complex. Upon gradual addition of TBAF, the signal due to the NH proton of secondary amine becomes broadened and finally vanished when almost 1 equivalent of F^- was added. When F^- ion was added beyond 1 equivalent, deprotonation

of the N–H protons and subsequent delocalization of the negative charge throughout the aromatic ring occurs, this process is facilitated due to the presence of electron withdrawing substituent at the para position to the phenyl ring. It is also seen that during the titration of the F^- ion, the N-H proton signal of the coordinated imine fragment at about 9.86 ppm remains almost stable up to 1 equivalent and it gets slightly broadened, with almost same chemical shift, when excess of F^- was added, indicating a very weak hydrogen bonding interaction with this imine (=N–H) proton. The chemical shift values of all the other aromatic protons remain unaltered during the titration.

Fig. 7

4.3. Absorption Spectral Changes of the Receptors upon Interaction with Anions

Changes in the Uv-vis spectra of the complexes in MeCN solution on addition of successively increasing amount of TBAF is shown in Fig. 8 and the changes observed during the titration is tabulated in Table 6. Complexes **1** and **2** show only minor changes on addition of TBAF, but the other four complexes (**3**-**6**) show appreciable spectral modifications, with generation of three isosbestic points at 390 nm, 485 nm and 510 nm. The Job's plot shown in the inset of the figures show that for all the four complexes F^- binds in 1:1 molar ratio. The association constants derived from non-linear curve fitting using equation (2) (Fig. S33) are given in Table 7. The association constant values were found to be reasonably high (logKa > 5) for complexes **3**-**6**, with complex **5** and **6** having the highest and lowest value respectively of the association constant. These values are one order of magnitude greater than those observed for free thiosemicarbazone ligands (Table S2) and the later results are consistent with some earlier reports [33b,34]. The detection limits were calculated to be of the order of 10^{-8}(M) for **3**, **5** and **6** and 10^{-7}(M) for **4** (Fig. S34, Table S1), and thus these four complexes can act as highly sensitive reagent for detection of F^-. The detection limits obtained for complexes **3**, **5** and **6** are much smaller than some of the free thiosemicarbazones and thus these Ru(II) complexes are more sensitive sensors of F^- than free thiosemicarbazones [35,67].

Fig. 8

Fig. 9

There are few reports of thiosemicarbazones or its complexes being used as sensor of fluoride ion and it is worthwhile to compare these results with that of ours. Thiosemicarbazones of

thiophen-2-aldehyde, furan-2-aldehydes and their various substituted derivatives have been found to behave as sensors of F^- with binding constants varying between 0.16-3.3×10^5 M^{-1} for the thiophen based molecules and 2.88-36.31×10^3 M^{-1} for furan based molecules, the former values being slightly greater and the latter an order of magnitude lower than those of our free thiosemicarbazone values [33b,34]. However, in both these works the sensing behaviour thiosemicarbazone molecules were not found to be F^- specific, rather they also act as sensors for acetate, cyanide and dihydrogen phosphate. A fluoride specific sensor behaviour was observed for napthaldehyde thiosemicarabzone in DMSO solution [35].Though the binding constant value is not reported in this case but the detection limit was reported to be 2.2×10^{-5} M, which is one thousand parts less than our Ru(II) complexes. *In situ* formed Fe(III) complex of napthaldehyde thiosemicarabzone was also shown to have specific binding affinity for F^- with the detection limit of 140μM [33a]. Selective sensing of F^- was also reported for bis(thiocrabohydrazone) with thiophen-2-aldehyde and furan-2-aldehyde in DMSO solution [33c] with the binding constant values being 2.91×10^5 and 5.5 ×10^4 M^{-1} respectively. Both F^- and CN^- in preference to other anions were detected by 4-(phenyl)thiosemicarabzone of 3,5-diodosalicylaldehyde, but unfortunately neither the binding constant values nor the detection limits were reported [32c]. Two thiosemicarabzone molecules appended to thioxanthone were found to be selective sensors for F^- and Hg^{2+} with detection limit in the range of 10^{-7} M [66]. From the above discussion it seems clear that our Ru(II) complexes are superior to other thisomicarbazone derivatives reported in the literature both in respect of binding constant values and detection limits as well as in terms of greater selectivity for F^-.

Table 6. Absorption Spectral Data for the Complexes in Acetonitrile

Complex	**λ_{max}, nm(ε/M^{-1} cm^{-1})**		
	without added anion	**with 1 equiv. of added fluoride ion**	**Δλ, nm**
1	271 (81280) 312 (87620) 381 (46736) 498 (37336) 661 (3756)	NA	NA

2	272 (77868) 311 (87210) 374 (48616) 498 (36046) 665 (3362)	NA	NA
3	271 (89960) 311 (101196) 375 (59768) 499 (46122) 662 (4170)	275(86115) 311(89536) 412(55926) 532(35810) 785(6677)	 37(375→412) 33(499→532) 123(662→785)
4	272 (82900) 311 (99206) 374 (55266) 498 (43960) 664 (4106)	276(81191) 311(83565) 404(49335) 541(26518) 792(3141)	 30(374→404) 43(498→541) 128(664→792)
5	270 (88848) 312 (95246) 375 (56356) 498 (42670) 659 (3860)	278(82509) 311(84689) 416(53901) 531(35383) 783(3838)	 41(375→416) 33(498→531) 124(659→783)
6	271 (98758) 312 (10678) 386 (59510) 498 (50466) 664 (4666)	273(93449) 311(93729) 400(52921) 543(26845) 790(3127)	 14(386→400) 45(498→543) 126(664→790)

Table 7. Association constants (K_a/M^{-1}) for **1–6** toward fluoride in Acetonitrile at 298K

Complex	From Absorption Spectra
1	NA
2	NA
3	2.89×10^5
4	2.19×10^5
5	4.90×10^5
6	1.39×10^5

4.4. Changes in the Electrochemical Behaviour of the Receptors upon Interaction with Anions

The electrochemical anion recognition and sensing features of **1-6** have also been evaluated by following the change in redox potential of the oxidation processes (Fig. 10) as a function of the addition of different anions using cyclic and differential pulse voltammetric techniques. With the

progressive addition of F^- to **3**, negative shift of the initial Ru(III)/Ru(II) potential, at 0.52 V to 0.17 V occurs. As the F^- ion concentration reaches 1 equivalent, the couple at 0.52 V is completely replaced by the new couple at 0.16 V, but no further change in the E° value was observed on further addition of F^- up to 5 equivalents. The ligand based reduction potentials of the complexes remain almost constant on addition of F^- up to 5 equivalents, as shown in Fig. S27. However, no identifiable shift in E° values occurs on the addition of other anions (Cl^-, Br^-, I^-, OAc^-, SCN^-, HSO_4^- and $H_2PO_4^-$) up to 8 equivalents in the acetonitrile solution of complex **3**. All the other complexes also show very similar type of response with fluoride. The strong hydrogen bonding of the free NH proton of thiourea group in the thiosemicarbazone ligands in **1-6** under the influence of the strongly basic F^- ion increases the electron density on the metal centre, which in turn decreases the metal centered oxidation potentials. Thus, in accordance with the colorimetric observations (see above), all the complexes (**1-6**) can also function as excellent electrochemical receptors for the selective recognition of F^-.

Fig. 11

4.5. Nature of Receptor-Anion Interaction

The observations made above from colorimetric, electrochemical and ^1H NMR measurements clearly suggest that F^- ion interacts strongly with the complexes (**1-6**) in 1:1 stoichiometry. Anion basicity in acetonitrile is expected to follow the order $F^- > OAc^- > H_2PO_4^-$, Cl^-, HSO_4^-, SCN^-, Br^-, I^- in agreement with the Hofmeister series [67,68]. Thus, fluoride as the most basic anion, induced spectroscopic changes for complexes **1-6**. It is also noted that except F^- ion such interaction is very weak for other anions like Cl^-, Br^-, I^-, OAc^-, SCN^-, HSO_4^- and $H_2PO_4^-$. Close resemblance of absorption spectrum of **3** in the presence of OH^- (Fig. S32), to that in the presence of F^- ion, suggests that metal coordinated phenyl thiosemicarbazone ligands in **1-6** get strongly hydrogen bonded with F^- ion and finally deprotonated to form mono-negative species in the presence of an excess of F^- ions (Scheme 3). The fact that the NMR signals of the free complex are very similar to the NMR signals in presence of excess F^-, except one of the N-H signal which is involved in the interaction, clearly show that the thiosemicarbazone ligand remains undissociated from the complex during its interaction with the F^-. Moreover, both Uv-vis spectroscopy studies show that when complex **3** is first deprotonated by addition of aliquots of tetrabutylammonium hydroxide, and then to this mixture triflic acid is added gradually, the

spectral change is reversed and finally the spectrum of the parent complex is obtained (Figs S36), clearly demonstrating the reversibility of the deprotonation process.

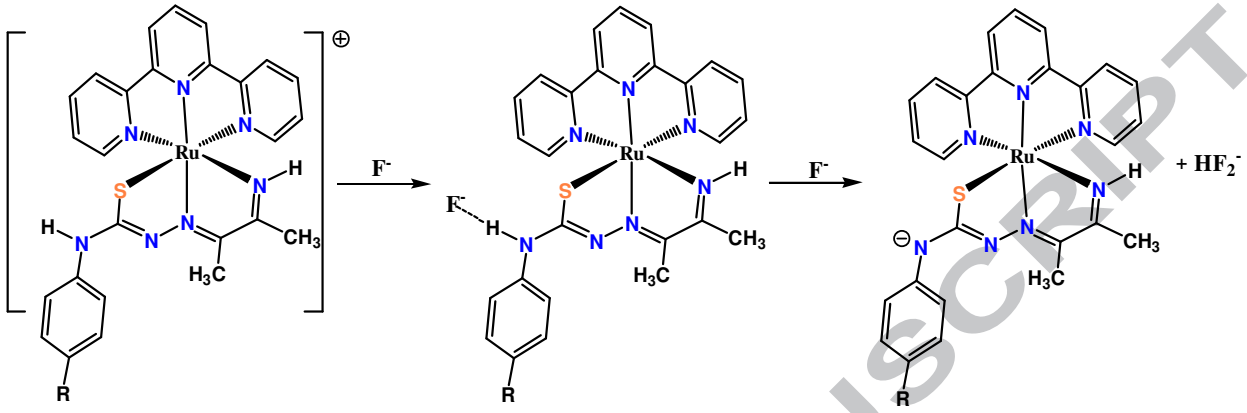

Scheme 3. Fluoride-Induced Coordination/Deprotonation Process of the complexes (**1-6**).

Conclusions

In this work we show that based on MLCT emission of Ru^{II}(trpy) as reporting unit and tridentate thiosemicarbazones as sensor unit very efficient multichannel fluoride detecting platforms can be designed. The fluoride ion can be estimated by Uv-Vis spectroscopy or by voltammtery. We also report here an interesting transformation of the parent hydroxyimino thiosemicarbzone to imino thiosemicarbazone during complexation with $Ru(terpy)^{3+}$. Though conversion of an oxime to imine during complexation has been previously reported in literature [50,51], most of them involve aldoxime and to our knowledge only one ligand system is known where a metal stabilized ketone imine complex was reported to be formed from the parent ketoxime [52,6]. Thus the present report is an important and interesting addition to the list of scarcely obtained ketone imine complexes generated from the corresponding ketoxime.

Acknowledgements

B.G. thanks Indian Institute of Engineering Science and Technology (IIEST) for an Institute fellowship. The authors acknowledge the All India Council for Technical Education (AICTE) for funding the purchase of a CH1106A potentiostat. The authors also acknowledge Saswati and Satabdi Roy, National Institute of Technology (NIT), Rourkela for the help in the NMR spectroscopy study.

References

[1] A. R. Cowley, J. R. Dilworth, P. S. Donnelly, A. D. Gee, J. M. Heslop, Dalton Trans. (2004) 2404.

[2] R. Pedrido, M. R. Bermejo, M. J. Romero, M. Vazquez, A. M. Gonzalez-Noya, M. Maneiro, M. J. Rodrıguez, M. I. Fernandez, Dalton Trans. (2005) 572.

[3] S. K. Chattopadhyay, S. Ghosh, Inorg. Chim. Acta. 131 (1987) 15.

[4] S. K. Chattopadhyay, S. Ghosh, Inorg. Chim. Acta. 163 (1989) 245.

[5] F. Bregant, S. Pacor, S. Ghosh, S. K. Chattopadhyay, G. Sava, Anticancer Res. 13 (1993) 1007.

[6] S. Grguric-Sipka, C. R. Kowol, S. M. Valiahdi, R. Eichinger, M. A. Jakupec, A. Roller, S. Shova, V. B. Arion, B. K. Keppler, Eur. J. Inorg. Chem. (2007) 2870.

[7] C. R. Kowol, E. Reisner, I. Chiorescu, V. B. Arion, M. Galanski, D. V. Deubel, B. K. Keppler, Inorg. Chem. 47 (2008) 11032.

[8] F. A. Beckford, M. Shaloski, Jr., G. Leblanc, J. Thessing, L. C. Lewis-Alleyne, A. A. Holder, L. Li, N. P. Seeram, Dalton Trans. (2009) 10764.

[9] B. Demoro, C. Sarniguet, R. Sánchez-Delgado, M. Rossi, D. Liebowitz, F. Caruso, C. Olea-Azar, V. Moreno, A. Medeiros, M. A. Comini, L. Otero, D. Gambino, Dalton Trans. 41 (2012) 1534.

[10] B. Demoro, R. F. M. de Almeida, F. Marques, C. P. Matos, L. Otero, J. C. Pessoa, I. Santos, A. Rodríguez, V. Moreno, J. Lorenzo, D. Gambino, A. I. Tomaz, Dalton Trans., 42 (2013) 7131

[11] M. Maji, M. Chatterjee, S. Ghosh, S. K. Chattopadhyay, B. M. Wu, Thomas C. W. Mak, J. Chem. Soc., Dalton Trans. (1999) 135.

[12] M. Maji, S. Ghosh, S. K. Chattopadhyay, T. C. W. Mak, Inorg. Chem. 36 (1997) 2938.

[13] D. Mishra, S. Naskar, Michael G. B. Drew, S. K. Chattopadhyay, Polyhedron 24 (2005) 1861.

[14] (a) F. Basuli, S. -M. Peng, S. Bhattacharya, Inorg. Chem. 36 (1997) 5645; (b) F. Basuli, M. Ruf, C. G. Pierpont, S. Bhattacharya, Inorg. Chem. 37 (1998) 6113; (c) F. Basuli, S. M. Peng, S. Bhattacharya, Inorg. Chem. 39 (2000) 1120; (d) I. Pal, F. Basuli, T. C. W. Mak, S. Bhattacharya, Angew. Chem. 113 (2001) 15.

[15] D. Mishra, S. Naskar, Michael G. B. Drew, S. K. Chattopadhyay, Inorg. Chim. Acta. 359 (2006) 585.

[16] S. Naskar, S. Naskar, Mike G.B. Drew, Serge I. Gorelsky, B. L. Kaiser, A. Aukauloo, D. Mishra, S. K. Chattopadhyay, Polyhedron 28 (2009) 4101.

[17] T. S. Lobana, R. Sharma, G. Bawa, S. Khanna, Coord. Chem. Rev. 253 (2009) 977.

[18] P. Sengupta, R. Dinda, S. Ghosh, W. S. Sheldrick, Polyhedron 22 (2003) 447.

[19] T. S. Lobana, G. Bawa, R. J. Butcher, Inorg. Chem. 47 (2008) 1488.

[20] (a) T. S. Lobana, G. Bawa, A. Castineiras, R. J. Butcher, M. Zeller, Organometallics 27 (2008) 175; (b) T. S. Lobana, G. Bawa, R. J. Butcher, B. -J. Liaw, C. W. Liu, Polyhedron 25 (2006) 2897; (c) T. S. Lobana, G. Bawa, R. J. Butcher, C. W. Liu Z. Anorg. Allg. Chem. **2009**, 635 (2009) 355.

[21] S. Blanchard, E. Bill, T. Weyhermüller, K. Wieghardt, Inorg. Chem. 43 (2004) 2324.

[22] S. Blanchard, F. Neese, E. Bothe, E. Bill, T. Weyhermüller, K. Wieghardt, Inorg. Chem. 44 (2005) 3636.

[23] G. S. Smith, B. Therrien, Dalton Trans. 40 (2011) 10793.

[24] S. K. Chattopadhyay, Ruthenium thiosemicarbazone complexes in *Ruthenium: Properties, Production and Applications, D. B. Watson (ed) Nova Science Publishers, Inc., New York***,** (2011) pp293-310.

[25] (a) X. Y. Liu, D. R. Bai, S. N. Wang, Angew. Chem. Int. Ed. 45 (2006) 5475; (b) W. J. Xu, S. J. Liu, X. Y. Zhao, S. Sun, S. Cheng, T. C. Ma, H. B. Sun, Q. Zhao, W. Huang, Chem. –Eur. J. 16 (2010) 7125; (c) P. Gamez, T. J. Mooibroek, S. J. Teat, J. Reedijk, Acc. Chem. Res. 40 (2007) 435; (d) M. Arunachalam, I. Ravikumar, P. Ghosh, J. Org. Chem. 73 (2008) 9144; (e) R. Dutzler, E. B. Campbell, M. Cadene, B. T. Chait, R. MacKinnon, Nature 415 (2002) 287; (f) H. Maeda, Y. Ito, Inorg. Chem. 45 (2006) 8205; (g) M. Arunachalam, P. Ghosh, Org. Lett. 12 (2010) 328; (h) F. Zapata, A. Caballero, A. Tárraga, P. Molina, J. Org. Chem. 75 (2010) 162; (i) X.-F. Shang, X.-F. Xu, BioSystems 96 (2009)165.

[26] (a) V. B. Bregović, N. Basarić, K. M. Majerski, Coord. Chem. Rev. 295 (2015) 80; (b) R. M. Manez, F. Sancenon, Chem. Rev. 103 (2003) 4419; (c) A. E. Hargrove, S. Nieto, T. Zhang, J. L. Sessler, E. V. Anslyn, Chem. Rev. 111 (2011) 6603; (d) V. Vajpayee, Y. H. Song, M. H. Lee, H. Kim, M. Wang, P. J. Stang, K.-W. Chi, Chem. Eur. J. 17 (2011) 7837; (e) P. A. Gale, Coord. Chem. Rev. 213 (2001) 79; (f) C. R. Bondy, S. J. Loeb, Coord. Chem. Rev. 240 (2003) 77; (g) P. D. Beer, P. A. Gale, Angew. Chem., Int. Ed. 40 (2001) 486; (h) A. Chakraborty, R. Gunupuru, D. Maity, S. Patra, E. Suresh, P. Paul, Inorg. Chem. Commun. 13 (2010) 1522; (i) A. Ghosh, B.

Ganguly, A. Das, Inorg. Chem.46 (2007) 9912 (j) L. S. Evans, P. A. Gale, M. E. Light, R. Quesada, Chem. Commun. (2006) 965.

[27] (a) Y. Bao, B. Liu, H. Wang, J. Tian, R. Bai, Chem. Commun. (2011) 3597; (b) S. Guha, S. Saha, J. Am. Chem. Soc. 132 (2010) 17674; F. M. Ashcroft, Ion Channels and Disease, Academic Press, San Diego, CA, 2000.

[28] (a) K. L. Kirk, Biochemistry of the halogens and inorganic halides, Springer, Berlin. (1991) 58; (b) M. Kleerkoper, Metab. Clin. North Am. 27 (1998) 441; (c) C.D. Geddes, Meas. Sci. Technol. 12 (2001) 53–58; (d) E. Kissa, Clin. Chem. 33 (1987) 253; (e) J. Aaseth, M. Shimshi, J. L. Gabrilove, G. J. Støa Birketvedt, Trace Elem. Exp. Med. 17 (2004) 83; (f) Y. Xie, B. N. Popov, Anal. Chem. 72 (2000) 2075.

[29] (a) D. Saha, S. Das, S. Mardanya, S, Baitalik, Dalton Trans. 41 (2012) 8886; (b) S. Das, D. Saha, C. Bhaumik, S. Dutta, S. Baitalik, Dalton Trans. 39 (2010) 4162; (c) D. Saha, S. Das, D. Maity, S. Dutta, S. Baitalik, Inorg. Chem. 50 (2011) 46; (d) D. Saha, S. Das, C. Bhaumik, S. Dutta, S. Baitalik, Inorg. Chem. 49 (2010) 2334; (e) C. Bhaumik, S. Das, D. Saha, S. Dutta, S. Baitalik, Inorg. Chem. 49 (2010) 5049; (f) C. Bhaumik, D. Saha, S. Das, S. Baitalik, Inorg. Chem. 50 (2011) 12586; (g) D. Maity, S. Das, S. Mardanya, S. Baitalik, Inorg. Chem. 52 (2013) 6820; (h) C. Bhaumik, D. Maity, S. Das, S. Baitalik, Polyhedron 52 (2013) 890.

[30] (a) A. Das, H. Agarwala, T. Kundu, P. Ghosh, S. Mondal, S. M. Mobin, G. K. Lahiri, Dalton Trans. 43 (2014) 13932; (b) A. Das, T. Kundu, S. M. Mobin, J. L. Priego, R. J. Aparicio, G. K. Lahiri, Dalton Trans. 42 (2013) 13733; (c) T. Kundu, A. Dutta Chowdhury, D. De, S. M. Mobin, V. G. Puranik, A. Datta, G. K. Lahiri, Dalton Trans. 41 (2012) 4484; (d) T. Kundu, S. M. Mobin, G. K. Lahiri, Dalton Trans. 39 (2010) 4232.

[31] (a) C. Saravanan, S. Easwaramoorthi, C. Y. Hsiow, K. Wang, M. Hayashi, L. Wang, Org. Lett. 16 (2014) 354; (b) A. Ghosh, B. Ganguly, A. Das, Inorg. Chem. 46 (2007) 9912; (c) D. A. Jose, P. Kar, D. Koley, B. Ganguly, W. Thiel, H. N. Ghosh, A. Das, Inorg. Chem. 46 (2007) 5576.

[32] (a) X. Peng, Y. Wu, J. Fan, M. Tian, K. Han, J. Org. Chem. 70 (2005) 10524; (b) Y. Wu, X. Peng, J. Fan, S. Gao, M. Tian, J. Zhao, S. Sun, J. Org. Chem. 72 (2007) 62; (c) S. Mathan Kumar, K. Dhahagani, J. Rajesh, K. Nehru, J. Annaraj, G. Chakkaravarthi, G. Rajagopal, Polyhedron. 85 (2015) 830; (d) A. Misra, M. Shahid, P. Dwivedi, Talanta 80 (2009) 532.

[33] (a) W. Lu, H. Jiang, F. Hu, L. Jiang, Z. Shen, Tetrahedron 67 (2011) 7909; (b) L. E. Santos-Figueroa, M. E. Moragues, M. M. M. Raposo, R. M. F. Batista, S. P. G. Costa, R. C. M. Ferreira, F. Sancenón, R. Martínez-Máñez, J. V. Ros-Lisa, J. Sotoa, Org. Biomol. Chem. 10 (2012) 7418; (c) S. L. A. Kumar, R. Tamilarasan, M. S. Kumar, A. Sreekanth, Ind. Eng. Chem. Res. 50 (2011) 12379.

[34] M. M. M. Raposo, B. Garcıa-Acosta, T. Abalos, P. Calero, R. Martınez-Manez, J. V. Ros-Lis, J. Soto, J. Org. Chem. 75 (2010) 2922.

[35] W. Lu, M. Zhang, K. Liu, B. Fan, Z. Xia, L. Jiang, Sens. Actuators B, 160 (2011) 1005.

[36] R. A. Leising, S. A. Kubow, M. R. Churchill, L. A. Buttrey, J. W. Ziller, K. J. Takeuchi, Inorg. Chem. 29 (1990) 1306.

[37] S. Ghosh, P. K. Ray, S. R. Saha, A. P. Koley, Ind. J. Chem. 23A (1984) 745.

[38] A. K. Nandi, S. Chaudhuri, S. K. Majumder, S. Ghosh, Acta Crystallogr. Sect. C. 40 (1984) 1193.

[39] S. Naskar, S. Naskar, H. Mayer-Figge, W. S. Sheldrick, M. Corbella, J. Tercero, S. K. Chattopadhyay, Polyhedron 35 (2012) 77.

[40] SADABS, version 2.03; Bruker AXS Inc.: Madison, WI, (2002).

[41] G. M. Sheldrick, Acta Crystallogr. Sect. A 64 (2008) 112.

[42] M. J. Frisch, G. W. Trucks, H. B. Schlegel, G. E. Scuseria, M. A. Robb, J. R. Cheeseman, G. Scalmani, V. Barone, B. Mennucci, G. A. Petersson, H. Nakatsuji, M. Caricato, X. Li, H. P. Hratchian, A. F. Izmaylov, J. Bloino, G. Zheng, J. L. Sonnenberg, M. Hada, M. Ehara, K. Toyota, R. Fukuda, J. Hasegawa, M. Ishida, T. Nakajima, Y. Honda, O. Kitao, H. Nakai, T. Vreven, J. A. Montgomery, Jr., J. E. Peralta, F. Ogliaro, M. Bearpark, J. J. Heyd, E. Brothers, K. N. Kudin, V. N. Staroverov, R. Kobayashi, J. Normand, K. Raghavachari, A. Rendell, J. C. Burant, S. S. Iyengar, J. Tomasi, M. Cossi, N. Rega, J. M. Millam, M. Klene, J. E. Knox, J. B. Cross, V. Bakken, C. Adamo, J. Jaramillo, R. Gomperts, R. E. Stratmann, O. Yazyev, A. J. Austin, R. Cammi, C. Pomelli, J. W. Ochterski, R. L. Martin, K. Morokuma, V. G. Zakrzewski, G. A. Voth, P. Salvador, J. J. Dannenberg, S. Dapprich, A. D. Daniels, O. Farkas, J. B. Foresman, J. V. Ortiz, J. Cioslowski, D. J. Fox, Gaussian, Inc., Wallingford CT, 2009.

[43] D. Becke, J. Chem. Phys. 98 (1993) 5648.

[44] G. A. Petersson, M. A. Al-Laham, J. Chem. Phys. 94 (1991) 6081.

[45] P. J. Hay, W. R. Wadt, J. Chem. Phys. 82 (1985) 299.

[46] P. J. Hay, W. R. Wadt, J. Chem. Phys. 82 (1985) 270.

[47] Y. Takano, K.N. Houk, J. Chem. Theory Comput. 1 (2005) 70.

[48] Y. Cui, H. -J. Mo, J. -C. Chen, Y. -L. Niu, Y. -R. Zhong, K. -C. Zheng, B. -H. Ye, Inorg. Chem. 46 (2007) 6427.

[49] (a) Y. Liu, B. -H. Han, Y. -T. Chen, J. Phys. Chem. B 106 (2002) 4678; (b) Y. Liu, B.-H. Han, S. -X. Sun, T. Wada, Y. Inoue, J. Org. Chem. 64 (1999) 1487; (c) C. Basu, S. Biswas, A. P. Chattopadhyay, H. Stoeckli-Evans, S. Mukherjee, Eur. J. Inorg. Chem. (2008) 4927; (d) L. Wang, X. -J. Zhu, W. -Y. Wong, J. -P. Guo, W.-K. Wong, Z. -Y. Li, Dalton Trans. (2005) 3235; (e) B. Valeur, J. Pouget, J. Bouson, M. Kaschke, N. P. Ernsting, J. Phys. Chem. 96 (1992) 6545; (f) Y. Liu, B. Li, C. -C. You, T. Wada, Y. Inoue, J. Org. Chem. 66 (2001) 225.

[50] A. K. Das, S.-M.Peng, S. Bhattacharya, J. Chem. Soc., Dalton Trans. (2000) 181.

[51] (a) I. Chakraborty, B. K. Panda, J. Gangopadhyay, A. Chakravorty, Inorg. Chem. 44 (2005)1054; (b) C. K. Pal, S. Chattopadhyay, C. Sinha, A. Chakravorty, Inorg. Chem. 35 (1996)2442.

[52] S. K. Singh, S. Sharma, S. D. Dwivedi, R. -Q. Zou, Q. Xu, D. S. Pandey, Inorg. Chem. 47 (2008) 11942.

[53] (a) V. Y. Kukushkin, D. Tudela, A. J. L. Pombeiro, Coord. Chem. Rev. 156 (1996) 333; (b) V. Y. Kukushkin, A. J. L. Pombeiro, Coord. Chem. Rev. 181 (1999) 147.

[54] A. J. L. Pombeiro, V.Y. Kukushkin in Comprehensive Coordination Chemistry II, Vol 1, pp 631-637; A. B. P. Lever (Editor), J. A. McCleverty, T. J. Meyer (Eds. In Chief), Elsevier, Amsterdam, 2005.

[55] A. E. Graminha, A. A. Batista, J. Ellena, E. E. Castellano, L. R. Teixeira, I. C. Mendes, H. Beraldo, J. Mol. Str. 875 (2008) 219.

[56] M. B. Smith, J. March, March's Advanced Organic Chemistry: Reactions, Mechanisms and Structure, sixth edition, Wiley Interscience (2007) 1263.

[57] A. R. Cowley, J. R. Dilworth, P. S. Donnely, J. W. Shore, Dalton Trans. (2003) 748.

[58] S. C. Bart, K. Chłopek, E. Bill, M. W. Bouwkamp, E. Lobkovsky, F. Neese, K. Wieghardt, P. J. Chirik, J. Am. Chem. Soc. 128 (2006) 13901.

[59] B. de Bruin, E. Bill, E. Bothe, T. Weyhermuller, K. Wieghardt, Inorg. Chem. 39 (2000) 2936.

[60] P. H. M. Budzelaar, B. de Bruin, A. W. Gal, K. Wieghardt, J. H. van Lenthe, Inorg. Chem. 40 (2001) 4649.

[61] S. Naskar, B. Pakhira, D. Mishra, P. Mitra, S. K. Chattopadhyay, S. Naskar, Polyhedron 100 (2015) 170.

[62] S. I. Gorelsky, E. S. Dodsworth, A. B. P. Lever, A. A. Vlcek, Coord. Chem. Rev. 174 (1998) 469.

[63] S. I. Gorelsky, A. B. P Lever, J. Organomet. Chem. 635 (2001) 187.

[64] A. B. P. Lever, S. I. Gorelsky, Coord. Chem. Rev. 208 (2000) 153.

[65] J.R. Dyer, Application of Absorption Spectroscopy of Organic Compounds, Prentice-Hall of India Pvt. Ltd., New Delhi. (1989) 37.

[66] L. Ding, M. Wu, Y. Li, Y. Chen, J. Su, Tetrahedron Lett. 55 (2014) 4711.

[67] F. Hofmeister, Arch. Exp. Pathol. Pharmakol. 24 (1888) 247.

[68] W. Kunz, J. Henle, B. W. Ninham, Curr. Opin. Colloid Interface Sci. 9 (2004) 19.

[69] M. Trivedi, S. K. Singh, D. S. Pandey, R.-Q. Zou, M. Chandra, Q. Xu, J. Mol. Str. 886 (2008) 136.

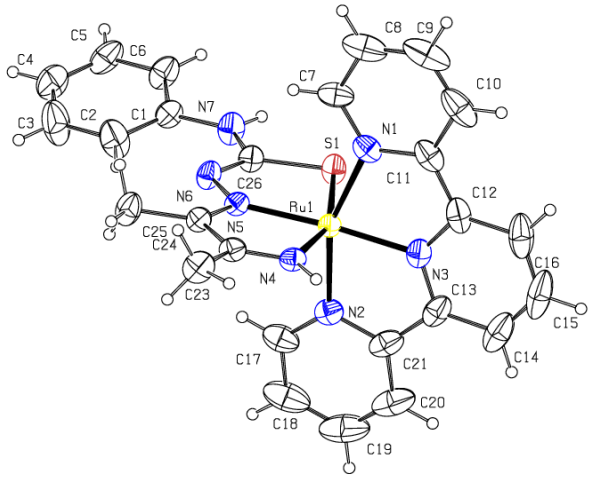

Fig. 1 ORTEP diagram (30% probability level) of complex **2**. Only the cationic complex part is shown in the figure. The PF_6^- anion and the solvent molecule ($CHCl_3$) are omitted for clarity of the figure.

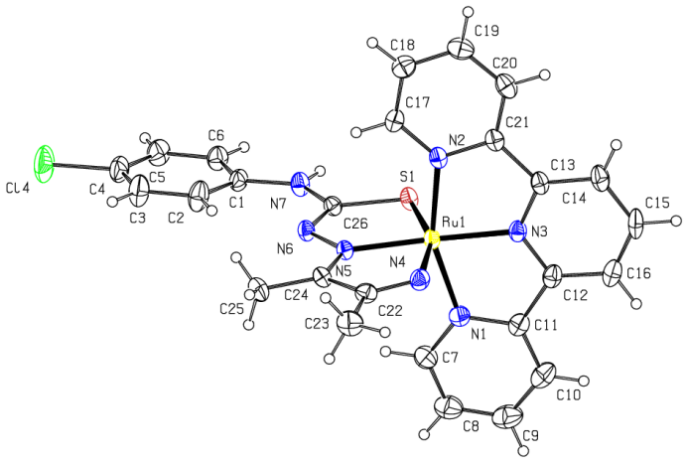

Fig. 2 ORTEP diagram (30% probability level) of complex **3**. Only the cationic complex part is shown in the figure. The PF_6^- anion and the methanol molecule are omitted for clarity of the figure.

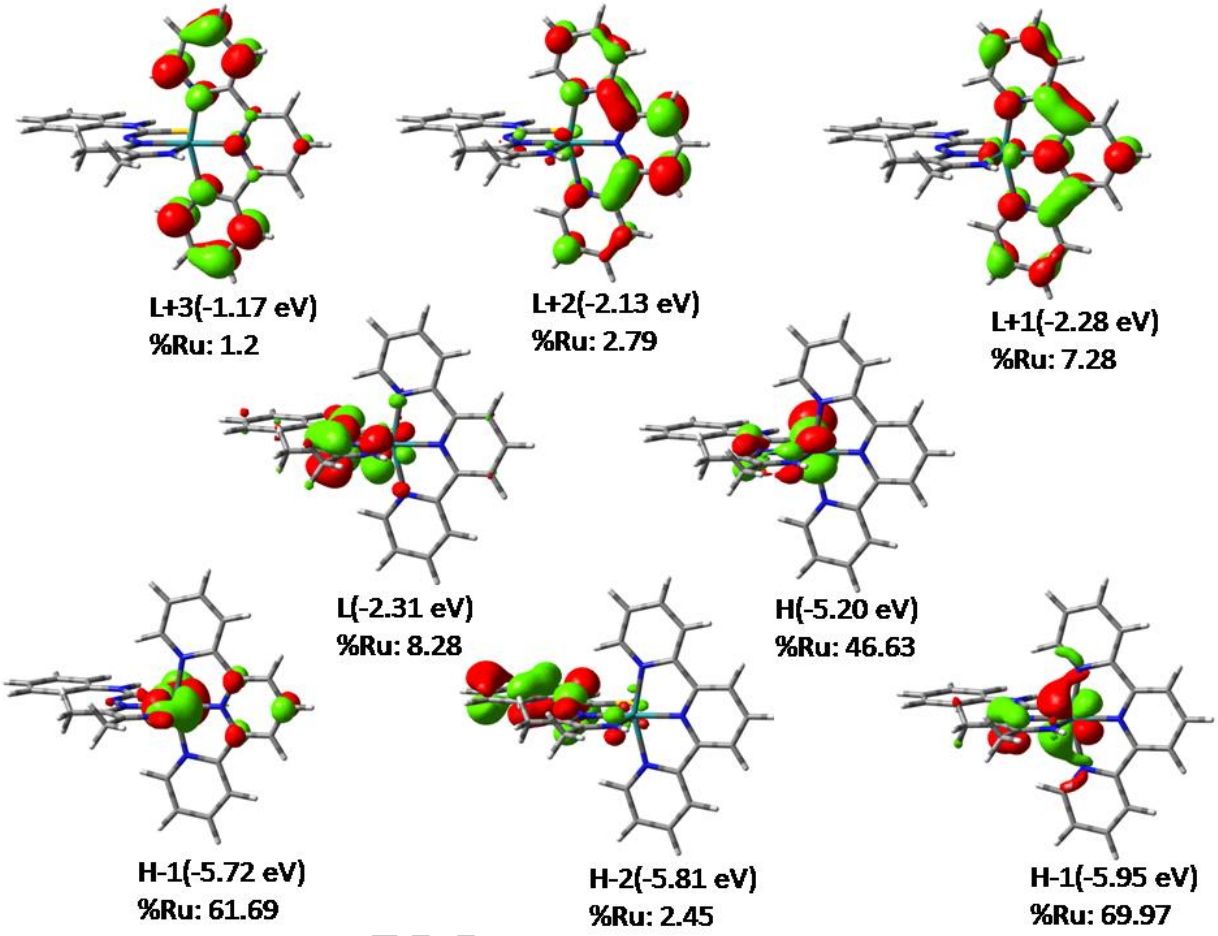

Fig. 3 Frontier orbitals of the complex **2** obtained by DFT calculations.

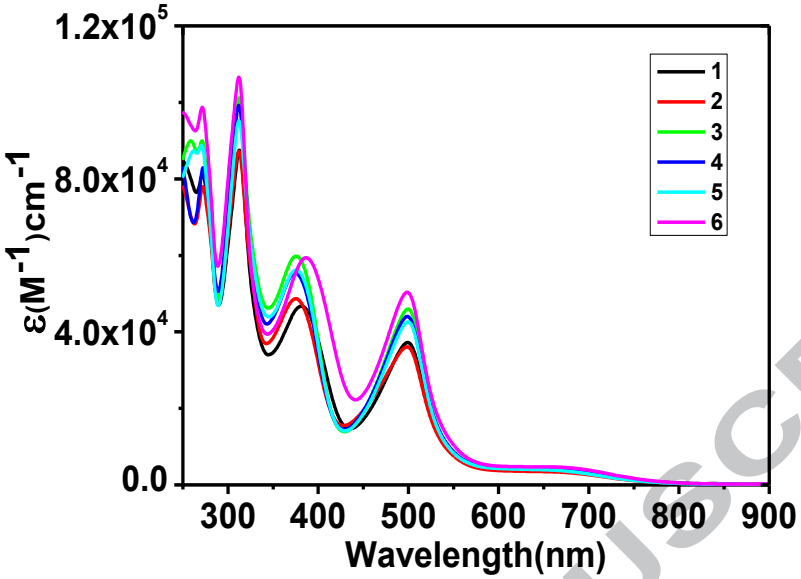

Fig. 4 Electronic spectra of equimolar solution of **1-6**, recorded in acetonitrile solution at room temperature (298 K).

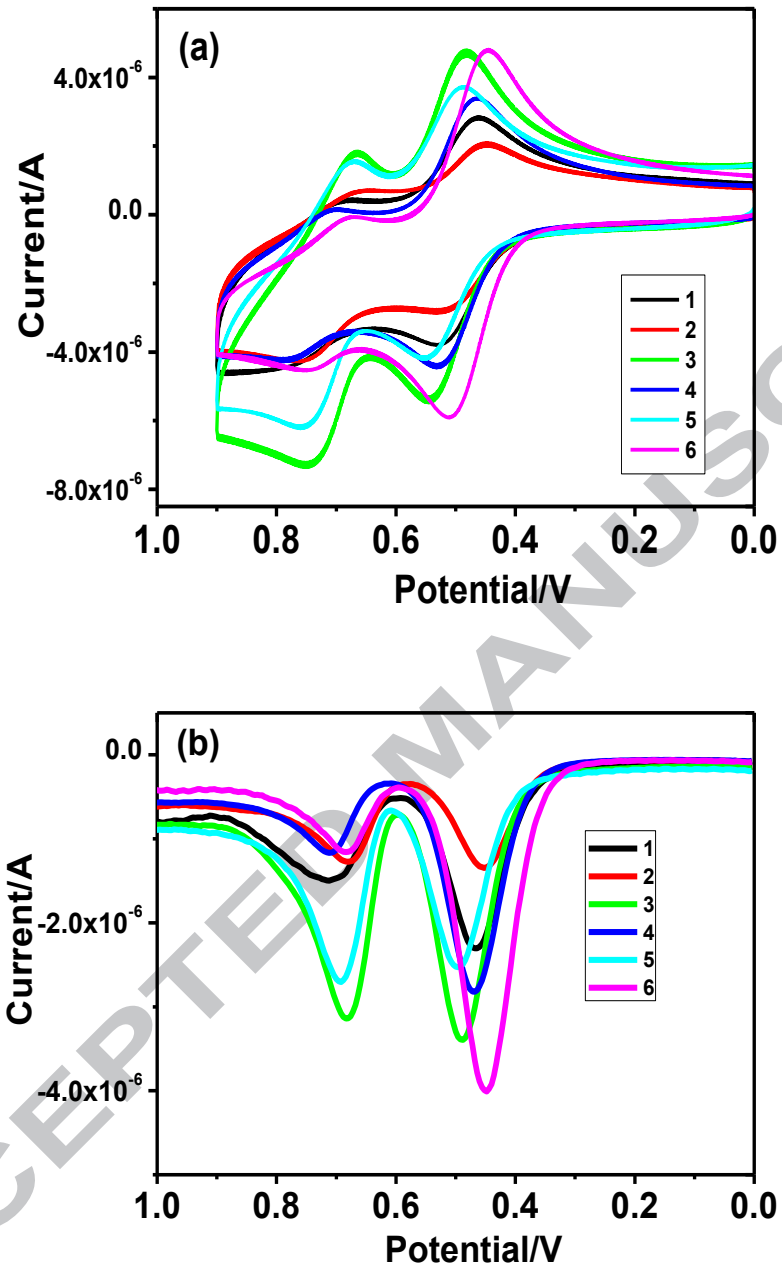

Fig. 5 a) Cyclic voltammograms and (b) differential pulse voltammograms overlay diagrams of **1**-**6** in the oxidative side, recorded in acetonitrile solution. Potentials are referred against Ag/AgCl/KCl(std.) electrode.

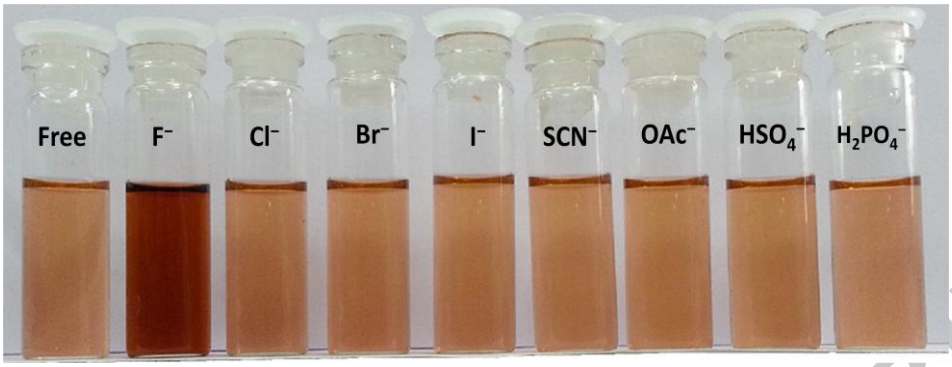

Fig. 6 The visual change in colour of complex **3** (5×10^{-5}M) in CH_3CN on addition of one equivalent of various anions as their tetrabutylammonium(TBA) salts.

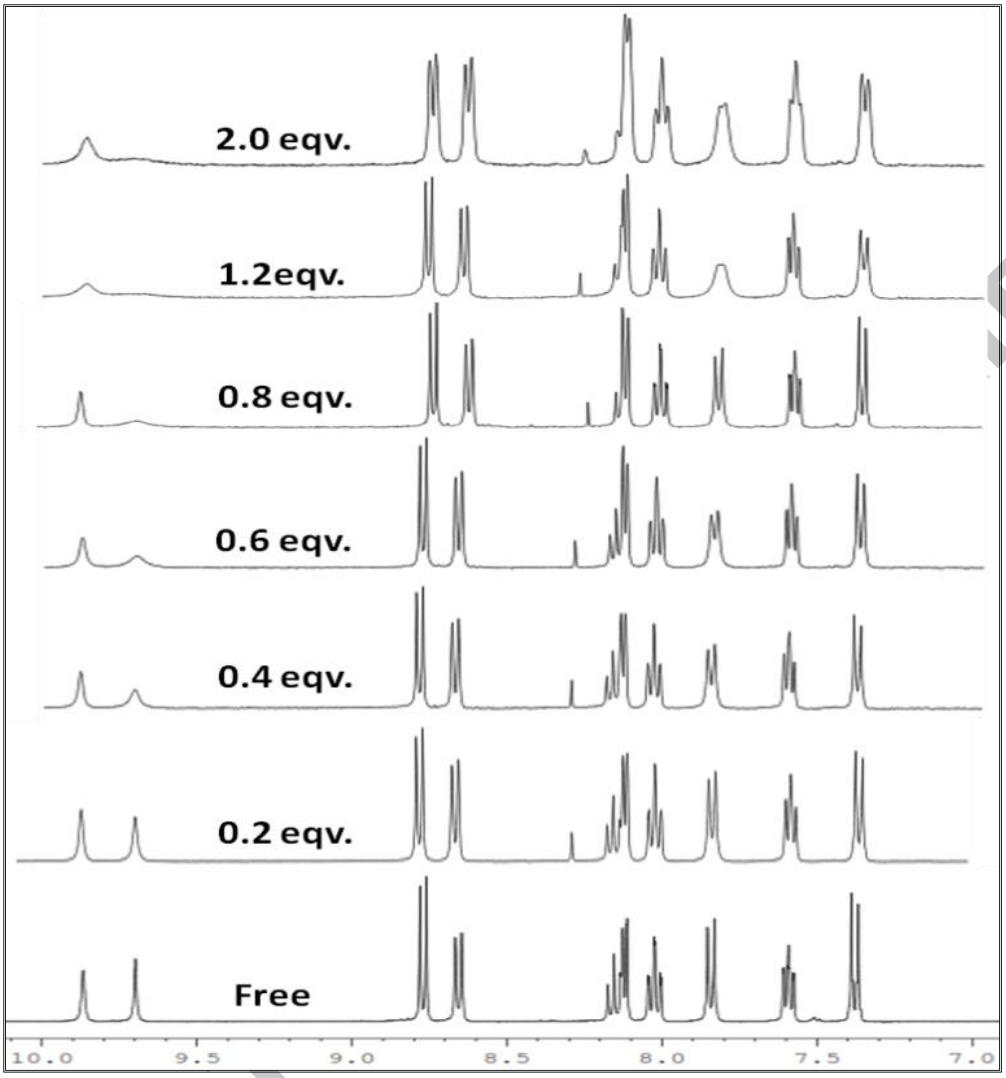

Fig. 7 ^{1}H NMR (400 MHz) titration of **3** in DMSO-d_6 Solution (5×10^{-3}M) on addition of incremental amounts of TBAF (0-2 equivalents).

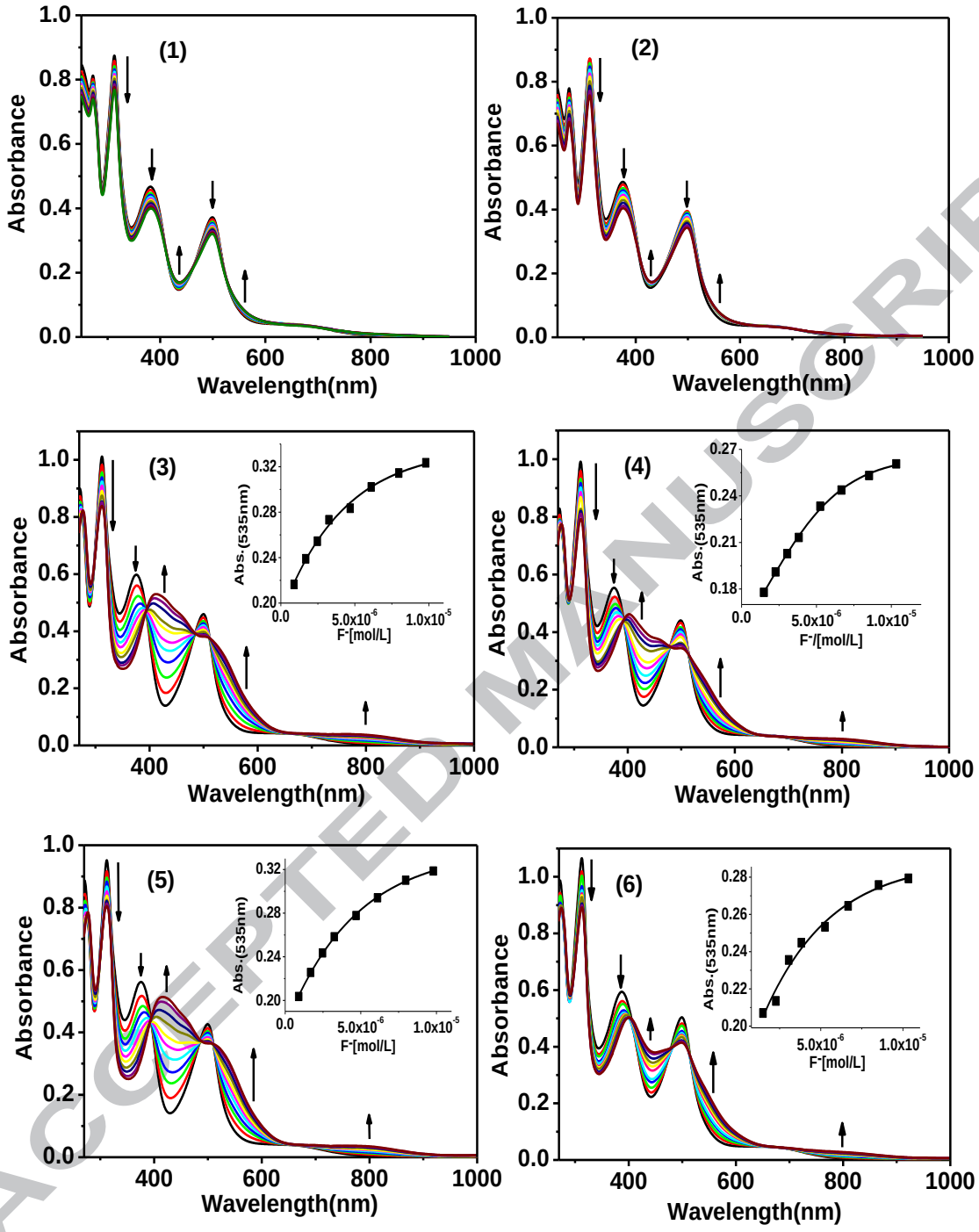

Fig. 8 Changes of the UV-vis spectra of **1**-**6** (1×10^{-5}M) in acetonitrile at 298K upon incremental addition of F^- ions from 0 to 1 equivalent. Inset shows the fit of the experimental emission data to a 1:1 binding profile.

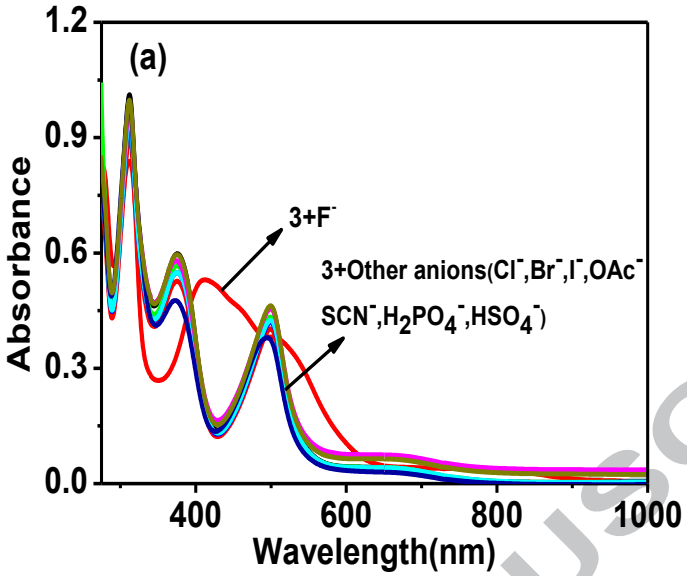

Fig. 9 Changes in absorption spectra of **3** in acetonitrile upon the addition of different anions as their TBA salts up to eight equivalents.

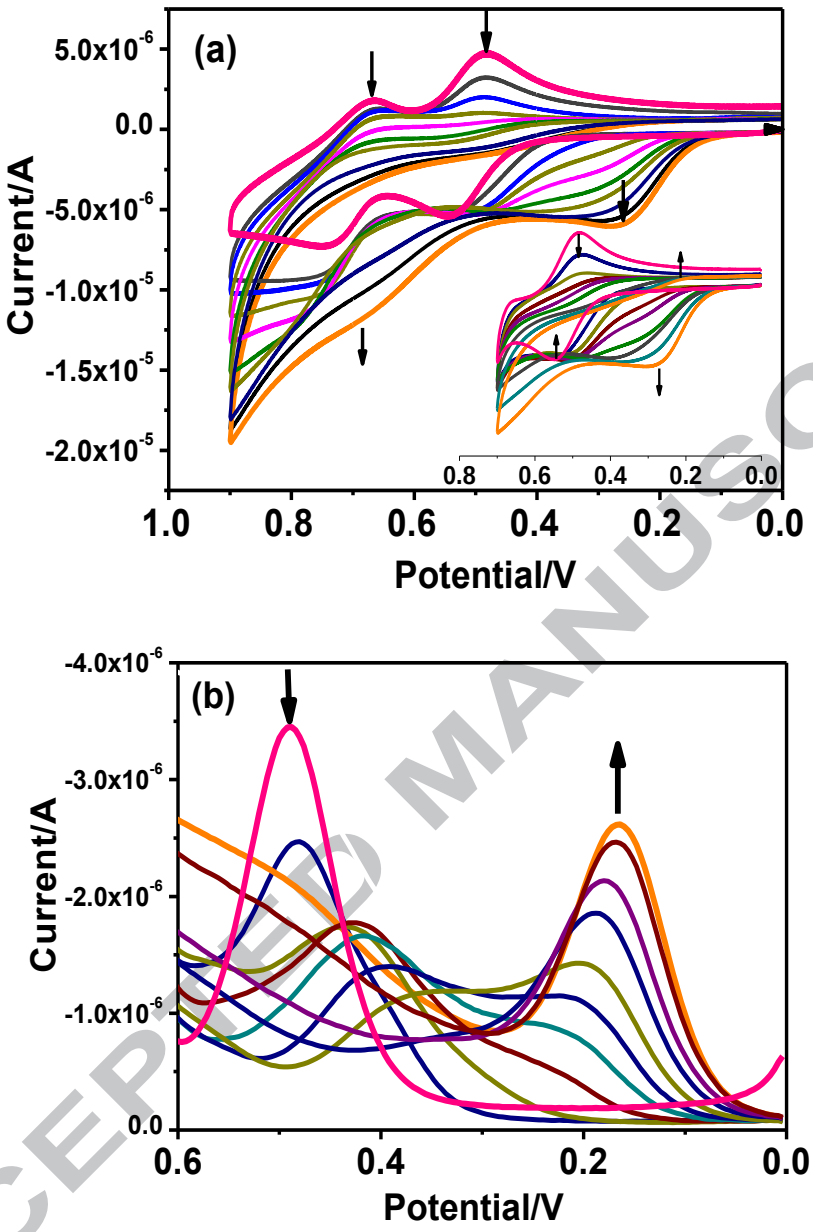

Fig. 10 Changes in the (a) cyclic voltammograms and (b) differential pulse voltammograms (oxidation couple only) of **3** (2×10^{-4}M) in CH_3CN upon the gradual additions of TBAF up to one equivalent.

Graphical Abstract Pictogram

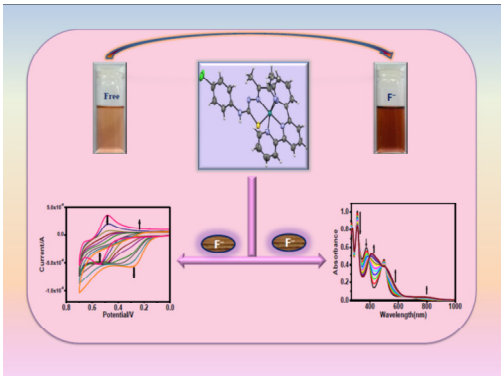

Graphical Abstract Synopsis

Ternary complexes of Ru(II) with terpy and six different tridentate thiosemicarbazone ligands are found to be excellent multichannel sensors for fluoride ion.

Research Highlight

- Ru(II) complexes with terpyridine and tridentate thiosemicarabzones are reported
- During complexation the oxime moiety of the ligands is converted to imine
- The complexes are excellent multichannel sensors for F^-